Report No. UMTA-CA-06-0088-80-1

AMTV HEADWAY SENSOR AND SAFETY DESIGN

A.R. Johnston
M. Nelson
P. Cassell
J.T. Herridge

Jet Propulsion Laboratory
California Institute of Technology
Pasadena, California
(JPL Publication 79-120)

JANUARY 1980

FINAL REPORT

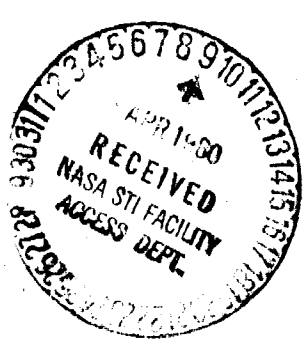

Prepared for

U.S. DEPARTMENT OF TRANSPORTATION

Office of Technology Development and Deployment
Urban Mass Transportation Administration
Washington, D.C. 20590

PREFACE

This report represents the combination of two efforts, one involving the design of the headway sensing system for an AMTV, and the second a study of techniques and concepts for building a safe AMTV body.

The headway sensor development and studies were conducted at Jet Propulsion Laboratory. The second-generation sensor hardware design and testing was made in combination with the previously developed experimental AMTV vehicle.

Conducted in parallel with the sensor hardware work was a study of alternative techniques for performing the headway sensing function. The point of view taken in this study was to examine the potential of each technique in the near future, rather than one of trying to foresee longer range research breakthroughs and project their implications. We hoped to put in proper perspective technologies which might be introduced in the 2-5 year time frame.

The safety study was performed at Battelle Memorial Laboratory, Columbus, Ohio, under the direction of Mr. John T. Herridge, under contract from Jet Propulsion Laboratory. It draws from a considerable experience at Battelle in vehicular safety technology, both experimental and analytical.

The authors wish to acknowledge the assistance of Mr. David Robb, who created the artistic design sketches found in Figures 5-5, 5-6, 5-7, 5-8 and 5-9. Mr. Robb was a student at the Pasadena Design Center when he began this work, and is now employed by Chrysler Corporation, Detroit, Michigan.

We also would like to acknowledge the help of G. Meisenholder for his advice and assistance during the course of this work, and R. Marks for his careful review of the report draft.

Finally, we thank R. Hoyler and D. MacKinnon of the Advanced Development Division, DOT/UMTA for their continuing support, and for their many helpful suggestions and comments.

CONTENTS

Figures

Tables

SECTION 1

SUMMARY AND CONCLUSIONS

In this report, progress on two related aspects of the development of an Automated Mixed Traffic Vehicle (AMTV) is described. The two tasks involve improvements to the headway sensing system, and development of AMTV body design concepts that will minimize the chance of injury to pedestrians or occupants in the unlikely event of a collision.

1.1 HEADWAY SENSOR IMPROVEMENT

The original headway sensors on the experimental JPL AMTV were replaced with an improved system using the same principle, that of optical proximity sensing in the near IR. The improved sensor system is an array of optical elements, arranged in source-detector sets, and coupled to appropriate electronics to deliver primary (8 meters) or secondary (2.5 meters) channel signals for vehicle speed control. The main goals were to sharpen the definition of the sensed area to $\pm$15 cm laterally, to within a range of 8 to 12 meters along the vehicle path, and to reduce the response time of the sensor output to 0.1 second. These goals were essentially met, although the image quality of the single element lenses used caused some detection of a retro reflector target beyond 12 meters. Functionally the array sensor performed well. Detection of cars parked at the side of the route and at several hundred feet ahead of the AMTV no longer occurs.

Turn-sensing was also investigated by adding single cruise-turn sensor elements and a U-turn element. Experiments were performed by manually (switch) enabling the turn channels, and yielded valuable insights into the requirements for turn sensors, but the single sensor elements can not provide an operational turn sensing capability.

A conceptual design for a simplified headway sensor, using an array of LEDs or detectors in the focal plane of a single lens to cover the required width of the AMTV path is presented. This concept can combine turn sensing with the straight-ahead function, and has fewer elements to adjust. A simple experiment to show feasibility was performed with favorable results.

Fail safe design ideas for the sensor proper are discussed, and various ways of taking advantage of the redundancy inherent in a multielement array are described.

Finally, alternative sensor concepts are examined. The alternatives include other forms of optical proximity sensors using lasers, laser range finders, imaging sensors, ultrasonic sensors, and radar.

The conclusions reached are as follows:

(1) An optical proximity sensor based on LED's and silicon PIN detectors can meet the requirements stated in Reference 1-1.

(2) The recommended configuration is a focal plane array using a few camera or projection type lenses, rather than many simple lenses. Such a configuration can handle both cruise-turn and straight ahead functions, as well as being far less time consuming to adjust than the present array.

(3) Adequate turn sensing will require the capability of sensing a width of path approximately equal to the vehicle width at 8 meters ahead. The minimum cruise turn radius will be set by the sensor capability rather than lateral acceleration (passenger comfort).

(4) Road fixed signals will be required to enable the turn sensing channels.

(5) The best candidate for a "smart" headway sensor (one locating quantitatively all potential obstacles, even those some distance to the side of the path) for development in the immediate future is the scanning laser range finder. Such a device could be developed with existing technology. The limitation is cost, not feasibility.

(6) The ultrasonic sensor is very attractive in terms of being inexpensive and simple, but suffers from inadequate beam definition for the AMTV headway sensor application. If techniques using transducer arrays were developed for obstacle location in three dimensions then ultrasonic sensing would become an interesting candidate. The basic technology for such an approach exists, but effort would be needed to ensure that the technique would work with multiple or distributed targets.

(7) The ultrasonic sensor is a good candidate for a U-turn sensor.

(8) A radar sensor would have limitations on beam definition similar to ultrasonic techniques, but could employ a similar phased array approach. However, a radar system would require more complex electronics and would be more expensive than its ultrasonic equivalent.

(9) Imaging sensors may ultimately provide the best approach toward obtaining a "smart" headway sensor. However, the processing requirements for obtaining real-time data from real scenes are beyond the present state of the art.

1.2 SAFETY DESIGN

Three topics are addressed in this section: pressure sensitive switches, a study of energy absorbing bumpers, and the development of AMTV body design concepts. Several promising contact sensor candidates were identified and the task proved very useful in regard to identifying potential impact scenarios (Ref. 1-2).

Initially, several very rough sketches illustrating bumpers and overall concepts were generated at Battelle to serve as "straw men" for review and discussion by the team as a group. These rough sketches in combination with a number of nicely stylized configurations furnished by JPL at the beginning of the study served as a good point of departure. Based on this early conceptual effort, three basic configurations were suggested: (1) an open bodied concept based on the present tram and (2) a custom semi-enclosed design of the same approximate size as the present tram.

It should be noted that any of the subject concepts or further hybrids of them may be viable candidates depending on the requirements of the actual application (e.g., actual traffic mix, operating speeds, control logic, etc.). It should also be noted that the design features selected for these basic concept vehicles are meant to represent a variety of design considerations and not design requirements. For example, it may be appropriate to either increase or decrease a suggested thickness of energy absorbing padding depending on subsequent changes in intended AMTV operating environment and/or control logic. Furthermore, the minimum thickness of padding or energy absorbing bumper stroke can be increased to provide considerable leeway in aesthetic treatment, etc., to satisfy user needs.

Three overall conclusions were reached as follows:

(1) Significantly attenuating impact forces and eliminating serious pedestrian injuries in the event of an unlikely (but potentially possible) accident at the projected AMTV operating speeds of 11 to 24 kph represents an achievable goal. The severity of pedestrian impact injuries is directly proportional to the speed at impact. With conventional passenger cars, the severity of impact tends to increase gradually with increasing speed up to about 32 or 40 kph and then increase at an increasing rate. Practical pedestrian safety oriented vehicle designs such as those selected for the AMTV have been demonstrated to be highly effective at impact speeds of 32 kph.

(2) Several unsophisticated sensors, switches, etc., exist which appear to be viable means of reliably satisfying the desired pedestrian contact functions.

(3) Some significant tradeoffs exist in terms of pedestrian safety versus occupant safety, overall system cost, development time, design strategy, aesthetics, desired level of safety system redundancy, etc. Final system optimization will require a careful analysis of the actual vehicle mission, application operating conditions, control logic strategy, etc., in combination with time and cost constraints for the associated development.

SECTION 2

INTRODUCTION

The Automated Mixed Traffic Vehicle, or AMTV (also called the Autotram) is a new concept in transit which, when fully developed, will offer a low-cost option for tram or feeder type applications. The concept involves automation of an appropriate vehicle type so that it will follow a predetermined route, including passenger stops. Existing roadway surfaces are used, rather than special dedicated guideways as in an Automated Guideway Transit (AGT) system, with their dominating capital costs. An example of a hypothetical future AMTV application is shown in Figure 2-1.

Our initial work on the AMTV idea resulted in the construction of a breadboard type AMTV (Ref. 2-1, 2-2) which was operated in an experimental mode carrying passengers on a test route at JPL. Subsequently, the results from these tests were reviewed and the functional design of an AMTV was discussed (Ref. 1-1). The question of safety was also examined in Reference 1-1, and a failure analysis made of an AMTV system.

The key technology which must be developed in order to make an AMTV possible is the headway sensing technology required to prevent collision with obstacles or other traffic, e.g., pedestrians, or possibly other vehicles which share the AMTV pathway.

Earlier developments in automated warehousing and similar systems* have similar vehicular control systems, but since they can operate productively at very low speeds (3 kph), mechanical cats-whisker contact switches can be used for headway sensing. In the AMTV speeds higher than normal walking speed would be used, so that a headway sensing range to about 8 meters is needed.

In addition to headway sensing, and no less important, good reliability and careful fail-safe design must be achieved in any automated vehicle system designed for public use.

This report deals with further progress in two related aspects of the AMTV development: first, improvement in headway sensor performance, and second, in AMTV body design considerations to make it safe for interacting with pedestrians and passengers.

A conclusion from the earlier AMTV technology and safety study (Ref. 1-1) was that the headway sensors should have a more sharply defined sensing area, and some quantitative requirements for the sensor were suggested.

In Section 3, the headway sensor developments are described.

An optical proximity sensor array was built to replace the first fan-beam type optics.

---

*Automated warehousing systems have been developed by a number of companies, including Control Engineering Corp., Pellston, Michigan, Barrett Corp., Chicago, Ill, and Lear-Siegler.

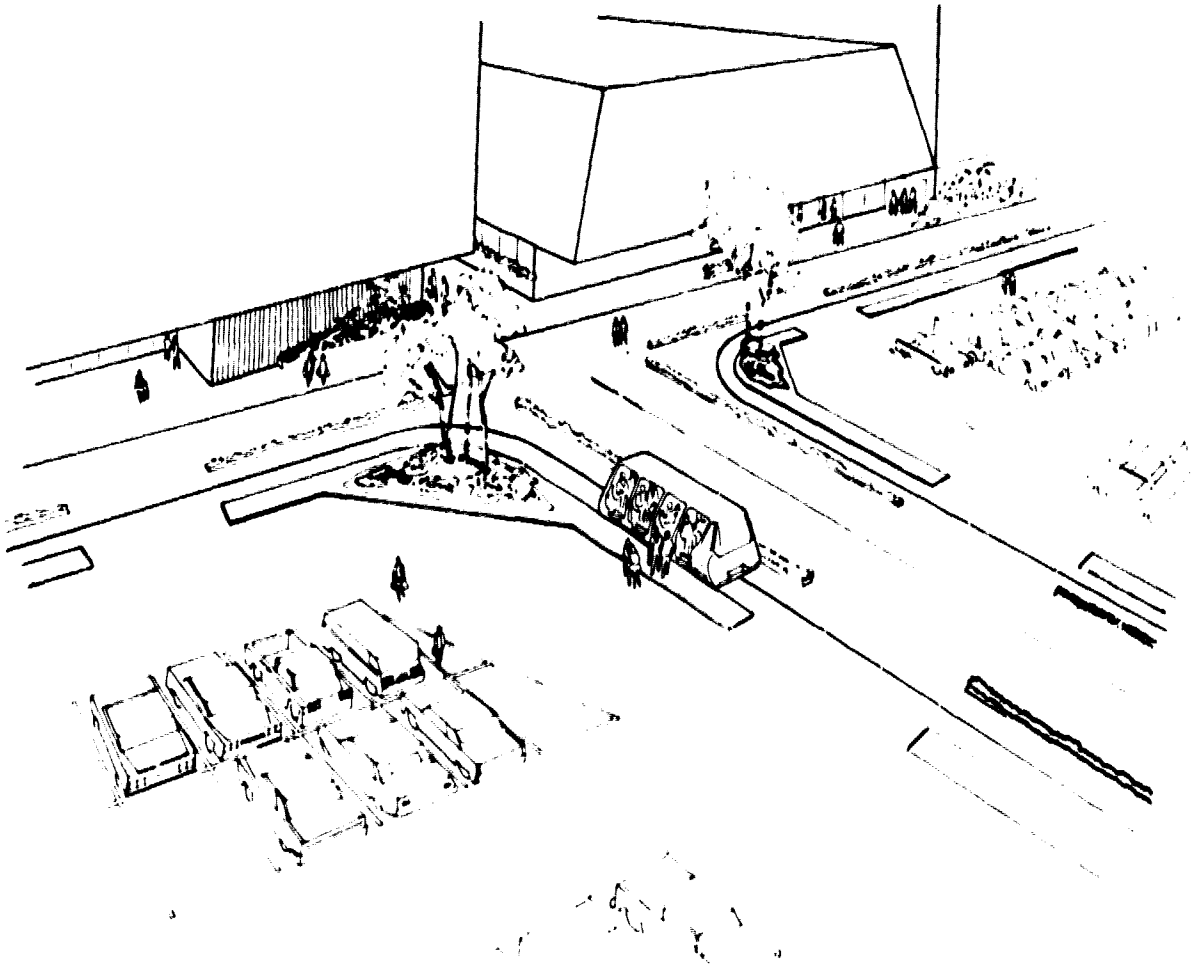

FIGURE 2-1. SKETCH ILLUSTRATING A POSSIBLE FUTURE AMTV APPLICATION

The new array sensor is qualitatively described, and results of road tests with it installed on the AMTV are briefly summarized in Section 3 below. Design details of the array sensor, and performance data are presented in Appendix A.

In addition, the need for special headway sensing in turns was identified. Initial turn sensing experiments were implemented and tests were performed. Design details and some test data are in Appendix B.

Calculation of the sensor output and its signal to noise performance are described in Appendix C. The calculations were compared with the observed signal to noise ratio in full sunlight. Also, some rather general curves are plotted from the calculations. These curves are useful in discussing power requirements and the noise versus response time limitations in optical sensing devices.

As a result of these experiments an improved implementation for an optical proximity array is described and recommended for future use. Rather

than an extended array of separate optical elements, this configuration involves using an array of detector (or LED) elements in the focal plane of a single lens. Fail safe design of the headway sensor is also discussed.

In Section 4, alternative concepts for headway sensing are discussed, using the present optical proximity sensor design as a baseline for comparison. Scanning laser proximity sensing, laser rangefinders, the use of imaging (TV) detectors, ultrasonic techniques, and radar are discussed. An ultrasonic sensor from a Polaroid camera was modified and tested with respect to the AMTV requirements. Design details of the modifications to the ultrasonic sensor, and the test results are reported in Appendix D.

Finally, in Section 5, the question of AMTV body design for safety is discussed. Minimizing the possiblity of injury to pedestrians in the unlikely event that a failure in the multiply redundant headway sensing system results in a collision receives particular attention. Sketches indicating possible design ideas for a future AMTV prototype body are presented.

SECTION 3

HEADWAY SENSOR DEVELOPMENT

This section describes the optical proximity sensor array which is currently incorporated on the JPL AMTV. Results of test runs on the AMTV route are briefly described. In addition, a simpler design using the array sensor concept is described. This design is called a focal plane array, and is recommended for future development because it can cover an area wider than the vehicle proper in a simpler way. Finally, the problem of providing a fail-safe sensing system is discussed.

The primary purposes of the present optical proximity sensor array development were to:

(1) Sharpen the definition of the sensed area, both laterally and along-track.

(2) Reduce the response time of the sensor to 0.1 second.

Both of these objectives were met, although the simple single-element lenses used were marginal in image quality, and the many opto-electronic elements were time-consuming to wire up and adjust.

3.1 HEADWAY SENSORS

3.1.1 Description

The JPL-AMTV second generation array sensor is patterned after the fan-beam proximity sensors used originally (Ref. 1-1). The array contains seven sensor elements, each made up of a light emitter consisting of a near IR (0.9μ) LED and collimating optics and two essentially identical receivers containing a silicon PIN detector arranged in a vertical column. In addition, two such elements, one on each side, are pointed outward at an angle for sensing objects while the AMTV is turning. At 8 meters from the sensor, the field-of-view (FOV) of the identical detector and source optics is about 15 cm in diameter. The intersection of the two fields-of-view creates a sensed volume, within which any object is illuminated by the light source and thus scatters light into the FOV of the associated detector.

The axis of one of the two receivers intersects the light source beam axis at a distance of 5 meters, creating the long range or primary sensor. The FOV of the other detector intersects the source beam at about 1.5 meters for the short range or secondary sensor. Since a single detector-emitter pair has a sensed volume only about 15 cm wide, the series of seven detector-emitter sets was used to cover the entire width of the vehicle. Detailed diagrams showing the geometry are presented in Appendix A.

Alternate elements, or columns of the array are inverted, four with the light source, as seen in Figure A-2, at the bottom and three with light source at the top. Such an arrangement permits a broader vertical coverage. The upper source beams are placed 1.25 meters above the road surface.

Signals from all upper beam elements in the array are combined into one TTL input to the control logic, and similarly all lower beam elements are combined into a separate TTL input, forming two independent primary and two secondary channels. Each sensor element (LED-detector pair) thus functions independently, and the common sensor circuitry is also duplicated, providing a high degree of redundance for the headway sensing system as a whole.

As was the case with the earlier sensor design, the proximity sensing concept requires that a certain threshold light power be detected in order to yield an output signal indicating an obstacle is present. A highly reflective target, such as a retroreflective automobile tail light lens will return more radiation from a given location than a flat black surface. Therefore, the sensed volume must be larger for the retroreflective target. Comparative data for these two types of targets are shown in Figures A-7 and A-8 in Appendix A. These figures show how much larger the sensed volume is for a retroreflector target.

The design data and test results indicate that the desired definition of the sensed area has been achieved. The dominant contribution to the remaining disparity is imperfect imaging by the inexpensive simple lens used in each array element.

The overall sensor response time is determined by a low-pass smoothing filter at the detector output, which has an 0.1 second time constant. The purpose of the filter is to restrict the pass band of the detector electronics in order to suppress detector noise, primarily from background light. A tradeoff is involved between response time and false detections due to noise. Further discussion and graphical information is found in Appendix C.

3.1.2 Results

The array type sensor system worked well on the AMTV during the test runs on the JPL route loop. Performance in these runs showed a marked improvement over the earlier sensor system. It does not see parked cars as it cruises by them, nor does it detect the reflective tail lights of other cars at an excessive distance while following them.

A drawback of the array type sensor design presently implemented is the need for an initial time consuming, tedious adjustment of the detector and emitter elements and of an internal reflector in each light source. There are nine detector-emitter sets and each set has eleven mechanical degrees of freedom requiring adjustment. Adjustment time may be the dominant cost consideration for an industrially produced array sensor. In addition, field replacement of a sensor element, or realignment after a minor bump or dent to the sensor area of the AMTV would involve further adjustment. For these reasons, the focal plane array configuration is discussed below in Section 3.3, as a simpler, more compact design.

3.2 TURN SENSING

3.2.1 Types of Turns

A requirement for a special headway sensing capability in turns was identified early in the AMTV development work. The path of the vehicle moves out of the area protected by the straight-ahead sensors when in a turn, and wider lateral coverage is needed for a much longer radius curve than might be expected.

A clear distinction should be made between cruise-turns and U-turns. Cruise turns are defined as those having a radius of curvature of 30 meters or larger, which are traversed at the 11 kph cruising speed. A smaller radius of curvature can be negotiated at 11 kph without discomfort from lateral acceleration, but it is desirable to limit the minimum radius of curvature on the AMTV route in order to ease the headway sensing requirements.

A U-turn is envisioned as a minimum radius turn, having a radius of 4.25 meters with the present AMTV, which must always be negotiated at a reduced speed. A U-turn would be used to reverse the course of the AMTV at the end of its route in minimum space, or it may also be appropriate for a right-angle turn at an intersection. The sensing requirement in a U-turn is quite different, as the entire side of the vehicle toward the inside of the curve is advancing laterally toward a stationary obstacle and thus must be protected. However, the slow vehicle speed simplifies the problem a great deal, because the stopping distance is of the order of 0.5 meter.

3.2.2 Turn Sensor Experiments

An elementary cruise turn sensor was implemented, consisting of an additional array element on each side of the AMTV, with its axis pointed outward at an angle of 8 degrees ($\sim$1 meter at 8 meters). The turn sensor optics can be seen in the photograph, Figure 2-2, between the outer two elements on each side. Either turn element could be selected by a manually-operated switch, and when enabled, its digital output is fed into the existing primary and secondary sensing channels. Further detail about the geometry and circuits are given in Appendix B.

Functional tests were made with the cruise-turn sensing element in operation on the AMTV. Members of the AMTV team served as test obstacles. A short section of the guidewire having approximately a 30 meter radius curve was used for the test. Although the turn sensor elements functioned satisfactorily, we found that the one element was not adequate because, as the AMTV moved forward, its beam swept laterally across the obstacle too rapidly to be effective. Instead, a turn sensor capable of covering a significant width, similar to the straight-ahead array, is required. Even though the single turn-sensing element cannot be said to be a functional sensing system, the experiments made with it were a very valuable step in understanding the requirements for turn sensing in an AMTV.

Similarly, a U-turn sensor was implemented using a fan-beam optical proximity sensor from the earlier headway sensing module. The design and measured sensing profiles are again given in Appendix B. The single

element operated satisfactorily, but again did not cover the full width of the path swept out by the side of the AMTV. Two such elements in parallel would be required.

A diagram illustrating two implementations of the U-turn sensing function is given in Figure 3-1. Measured profiles using two fan-beam optical sensors are shown in Figure 3-1a. Coverage for stationary obstacles is obtained, but it is possible for a pedestrian to move into the area behind the sensor pattern and be forced to step back when the AMTV moves.

An alternate U-turn sensor implementation based on an ultrasonic device, rather than the optical sensors, is shown in Figure 3-1b. A measured beam profile for the ultrasonic sensor described in Appendix D is superimposed to scale on the AMTV U-turn sketch. Sensor placement at the rear of the AMTV provides needed coverage along the side of the vehicle. No experiments have yet been performed on the AMTV with the ultrasonic device.

Since the entire side of the vehicle may need protection very short range sensing techniques, such as capacitive devices, or contact switches may also be considered in the future for the side surface of the AMTV to supplement the headway sensing system in U-turns.

3.2.3 Conclusions

Our experiments with turn sensing techniques lead to the following conclusions:

(1) As noted previously, a road-fixed signal will be required to enable the appropriate sensing channel. Four channels could be used, left and right cruise turn, and left and right U-turn. It is not sufficient to derive the enabling signal directly from the AMTV steering angle, because primary cruise-turn sensing must be initiated 8 meters before the AMTV reaches the curved section. If this is not done, the initial part of the curved path reaching from the start of the curve to the primary sensor cutoff at 8 meters will not be covered properly.

(2) Cruise-turn sensors must be able to cover the full width of the vehicle path for all curve-radii used. Primary and secondary channel coverage must extend to the same down-track distances as in the straight-ahead array. A diagram showing the geometry for a 30 meter radius curve is shown in Figure 3-2. The diagram helps to visualize the required coverage. The additional width of coverage required at 8 meters distance in the curve is essentially equal to the width of coverage (2 meters) required for the basic or straight-ahead headway sensors. Since the added coverage required is continuous from the edge of the straight-ahead pattern, the turn sensor profile shown on the figure would handle all curve radii greater than 30 meters.

(3) The focal plane array implementation described in the following section of this report could incorporate the

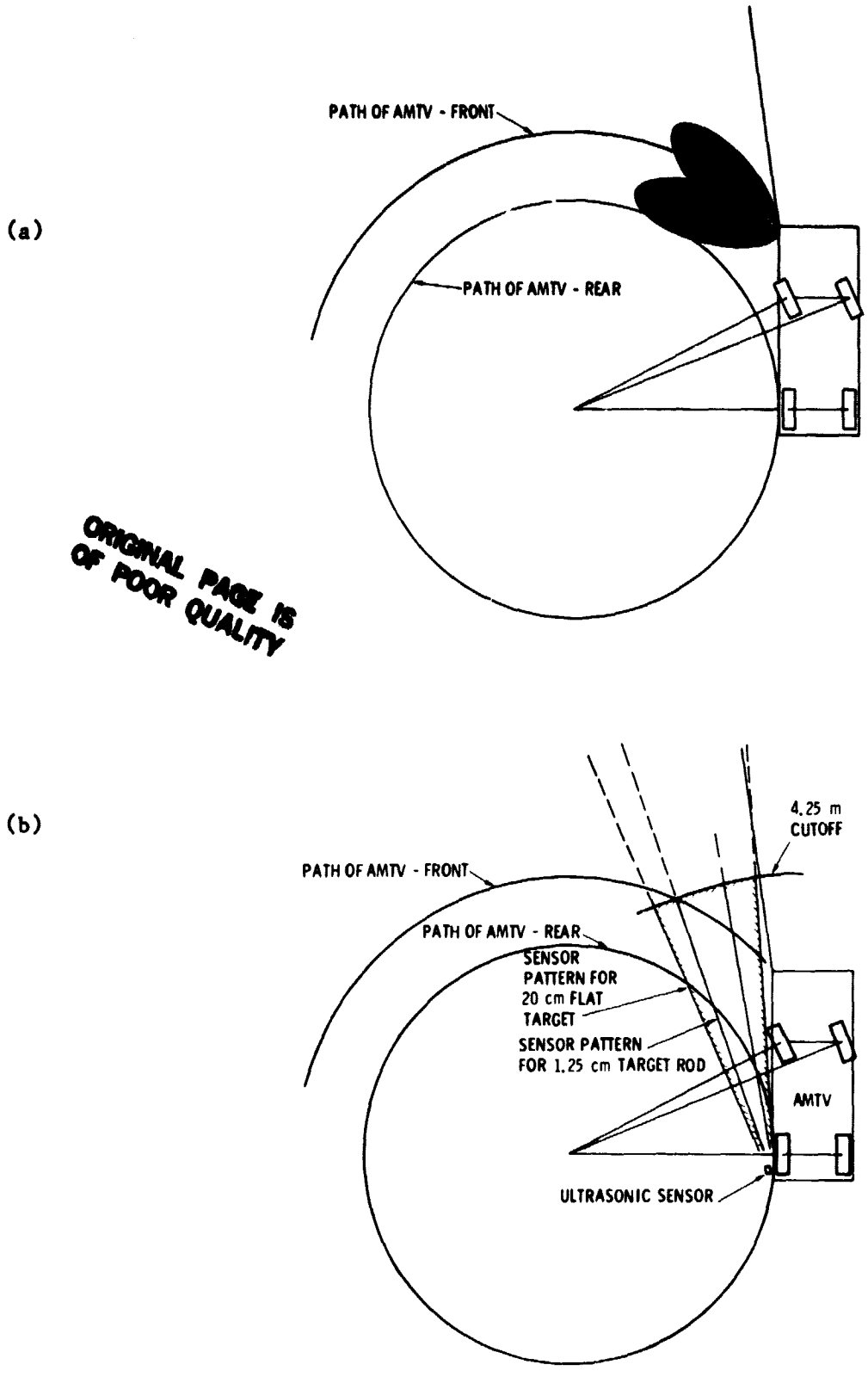

FIGURE 3-1. GEOMETRY OF (a) AN OPTICAL U-TURN SENSOR AND (b) A U-TURN SENSOR USING ULTRASONIC SENSING DEVICE

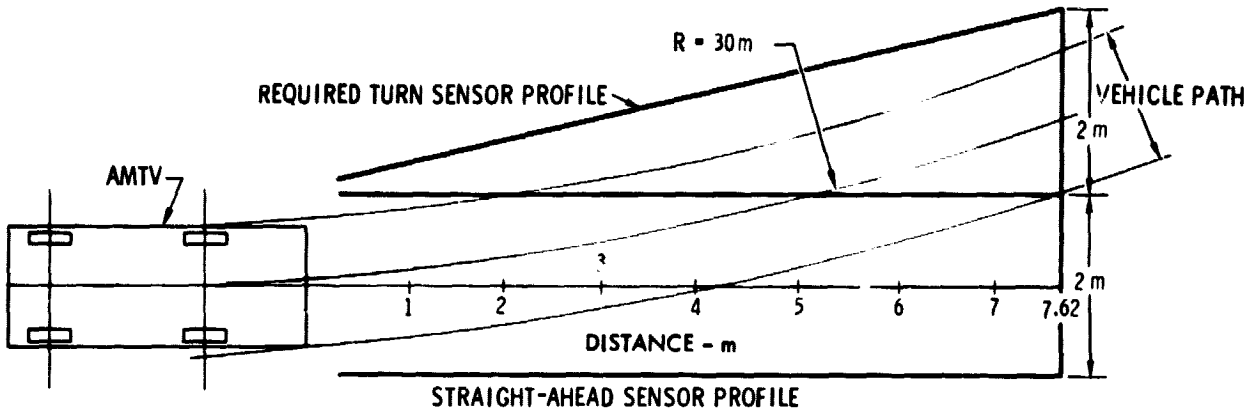

FIGURE 3-2. DIAGRAM SHOWING REQUIRED SENSOR PROFILE FOR 30 METER RADIUS CURVE

cruise-turn function. Additional light sources and detectors would be required in a focal-plane module for the turn function, but the external configuration and optics would not be changed.

Another possible implementation would be to mechanically point the basic straight-ahead sensor in the direction of the curve. An appropriate time-dependent pointing program, initiated by the road-fixed signal would be needed. The choice between these approaches appears to be an engineering consideration which is beyond the scope of this report.

(4) Appropriate constraints on route layout will have to be observed in order to ensure that the curve sensing design is compatible with the curve radii used. The suggestion made here, consistent with Figures 3-1 and 3-2, is to restrict cruise-curves to $R \geq 30$ meters, and to use $R \simeq$ 3-4 meters for slow maneuvers. Radii between 4 feet and 30 meters would not be used, or if the route environment dictated using a radius in this range, then that curve would have to be negotiated in the slow (3 kph) mode. Since the width of the sensor profile would be doubled with a turn sensor enabled, adequate clear space must be provided at curves to avoid slowing from a primary channel input.

3.3 FOCAL PLANE ARRAY SENSOR

An alternative headway sensor design, which places an array of detectors in the focal plane of a common lens, and a corresponding array of LED sources in the focal plane of another lens, is discussed in this section. Such a configuration is recommended for future development because it could

have essentially equivalent performance with far fewer separate components in the vehicle, and it also could incorporate the turn sensing function without great increase in complexity.

The simple lenses repeated in each horizontal line of the array sensor would be replaced with one camera or projection type lens able to image sharply over a large angular field. Then, instead of using separately adjustable mountings to position each detector or illuminator field-of-view, one can place the individual detectors or LED's in the focal plane of the wide-angle lens such that the desired coverage is obtained.

The advantage of this design approach is that the desired beam pattern can be built into a focal-plane module using normal machine-shop tolerances and it can easily be reproduced during fabrication. Better definition of the optical beam geometry can be obtained, because the image quality of a camera lens is considerably better than the simple lenses being used now. A focal plane aperture can be used for control of the detector and source field of view, which in turn define the sensed area.

The focal plane array configuration can cover a sensed area wider than the vehicle with good definition. To do so with the present array design requires a proliferation in the number of elements in the array.

Conceptually, the focal plane array sensor would take on the form shown in Figure 3-3. The optical elements would be placed in two columns, one near each side of the vehicle. The top and bottom elements would be light sources, while the intermediate two elements would contain IR detector arrays. The optics would be configured to cover an area 2 meters wide, approximately 30 cm on each side wider than the vehicle itself. The source beams would be placed, one at a height of 1.2 meters above the surface (at truck bed height) and the other at 0.3 meter to cover as nearly as possible to the road surface. Figure 3-4 shows a side view of the four components of one of the sensor columns in approximately the correct proportion.

Figure 3-5 is a conceptual drawing of a typical opto-electronic package. The illuminator package element is mechanically and optically similar to the detector package. The lens is a camera lens, having the parameters indicated in Table 3-1, and the housing has the proportions of a camera.

A shaped aperture would be cut in a thin metal stop placed in the focal plane of the lens, and focussed in the sensed field in front of the vehicle, to sharply define the distance to which a return can be detected as a function of horizontal angle. The design would use the same approach that has been employed on a point-by-point basis in the present array sensor.

The individual LED or detector components would be mounted immediately behind the focal plane aperture as shown in the figure. The elements in the focal plane, including the focal plane stop, and the individual detector or LED elements, would be fabricated as a unit, in a reproducible way. Thus, the formation of the beam geometry would be built into the device. Only the pointing of the unit as a whole must be done on the vehicle.

A breadboard of a source and a detector element of a focal plane array were built and tested in the laboratory to show feasibility of the concept. A single LED and a single detector were used. Each was moved to a new position in the focal plane for each data point, instead of fabricating a complete array, permitting a realistic test to be done with a minimum of effort devoted to fabrication. The results of the test are plotted in the form of a threshold profile in Figure 3-6, showing good discrimination between black and retroreflective targets, and confirming that an accurately shaped profile can be generated away from the axis of the sensor elements.

3.4 FAIL SAFE DESIGN TECHNIQUES

3.4.1 Background

Since proper functioning of the headway sensor system is vital to the safe operation of an AMTV, consideration must be given to fail-safe principles in its design. In this section, several approaches to realizing a reliable sensor system are presented. The question of fail-safe design will be addressed in terms of the optical proximity sensor array since it is the design we have experience with. Some of the techniques to be described are already incorporated in the present AMTV sensors.

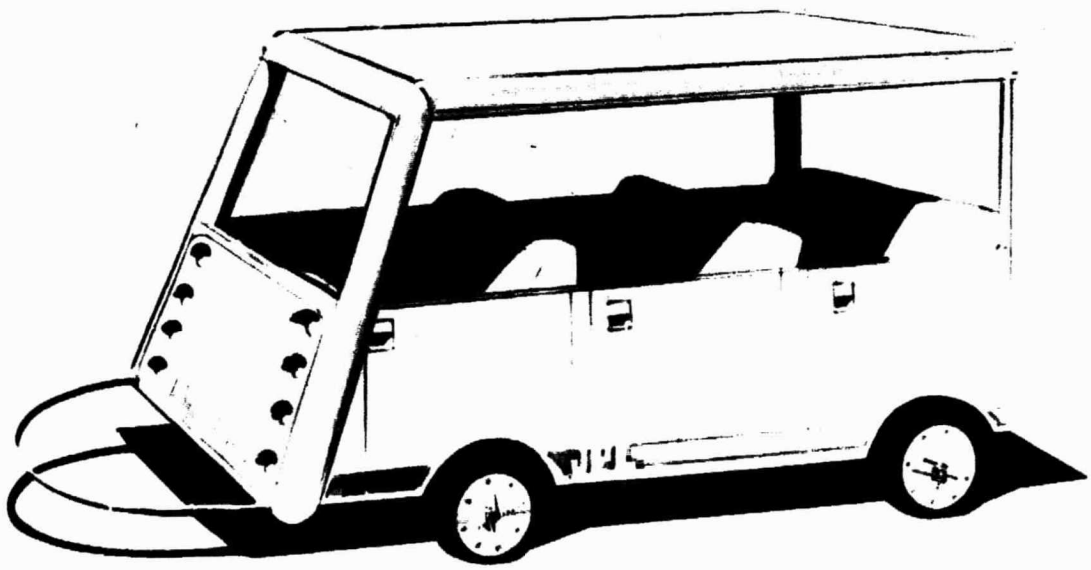

FIGURE 3-3. A POSSIBLE CONFIGURATION OF THE FOCAL PLANE ARRAY OF THE HEADWAY SENSING SYSTEM

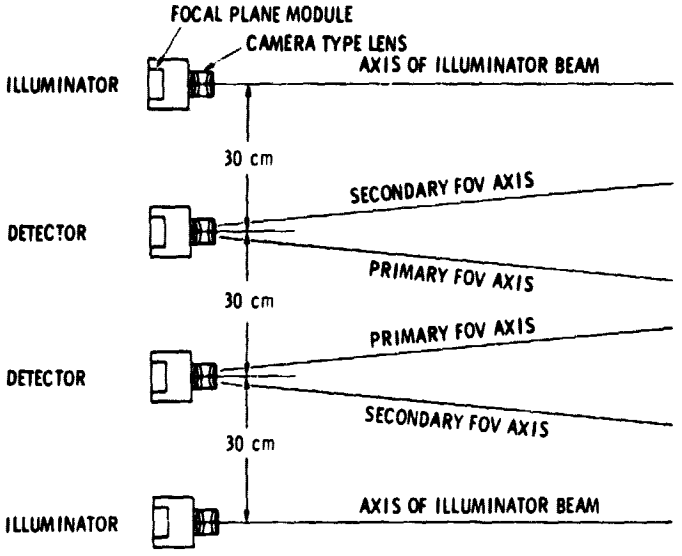

FIGURE 3-4. FOCAL PLANE ARRAY SENSOR CONFIGURATION WITH UPPER AND LOWER ILLUMINATOR BEAMS

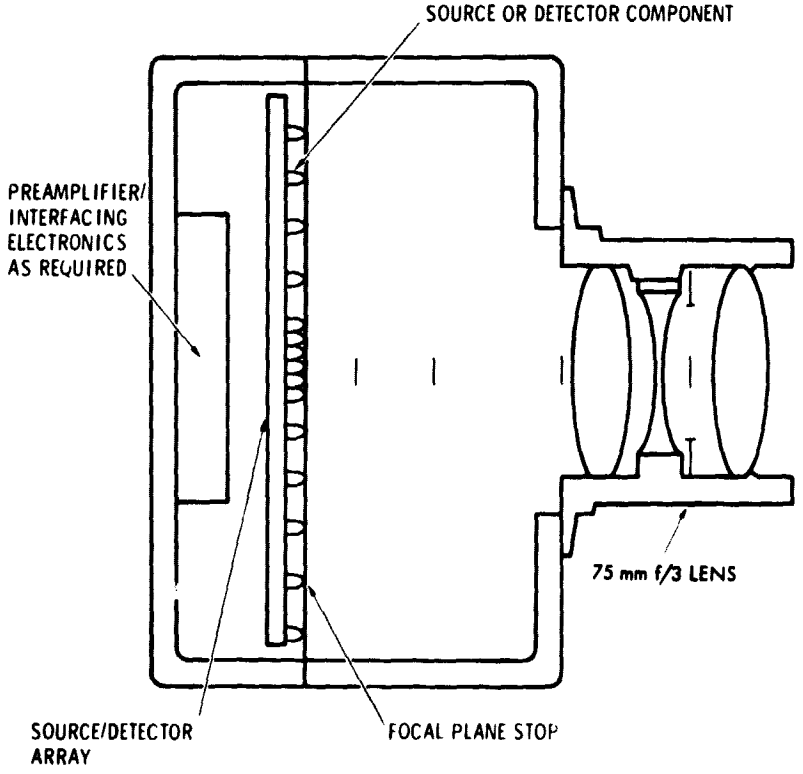

FIGURE 3-5. BASIC ELEMENT OF FOCAL PLANE ARRAY SENSOR

TABLE 3-1. LENS PARAMETERS

Diameter	3.1 cm
Focal Length	75 mm
Relative Aperture	f/2.4
Central Field of View	
Angular	10 deg
Linear	1.32 cm
Resolution	0.051 cm in central field of view
Extreme Field of View	
Angular	36 deg, center to edge
Linear	5.6 cm, center to edge

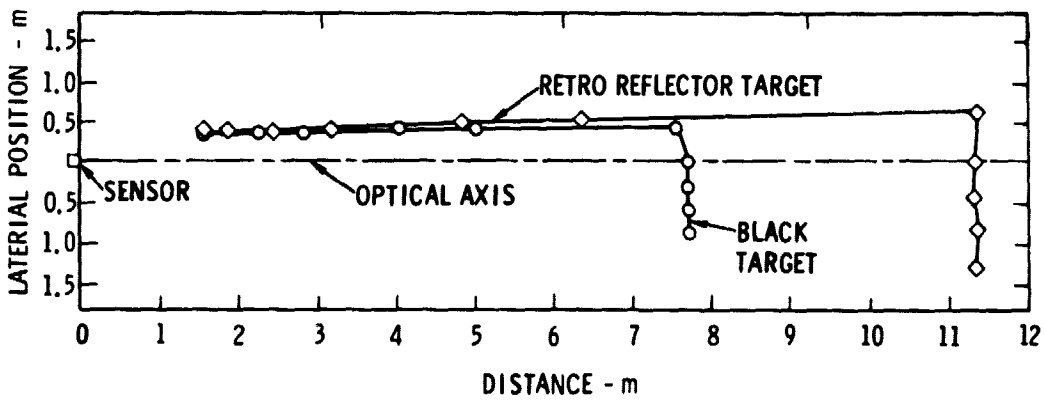

FIGURE 3-6. DETECTION THRESHOLD FOR BREADBOARD FOCAL PLANE ARRAY SENSOR EXPERIMENTS

The critical safety-related failure is the failure of an LED or any other failure in the direct signal channel which prevents detection of a return signal and can thus be considered equivalent to failure of an LED. Since an all-clear condition is indicated by the absence of any return, it is not possible to use something like a signal strength monitor to provide a functional check.

The suggested approach is to provide multiple redundancy in the sensor hardware design through the several independent sensor elements, together with appropriate function checks, made at frequent enough intervals to ensure reliability. If a failure occurs in such a redundant design, the results will in general, be degraded performance rather than a catastrophic failure.

The existing array sensor shown in Figure A-1 employs redundant design, but it has not yet been fully developed from the point of view of providing a fully fail-safe capability.

Redundancy can also be provided by the use of different types of sensors, for example, an ultrasonic sensor in combination with an optical proximity sensor. The use of completely independent and dissimilar components and circuits in this case could enhance the value of the redundant hardware. The combination of optical sensors and contact switch used on the present AMTV also provides redundancy, but the protection given by the contact switch by itself is a limited backup protection function.

Multiple redundancy in the sensor design must be supplemented by some procedure or indicator to signal that a failure has occurred. A periodic function test of the sensor is suggested for this purpose. Another possibility is to implement a self-check capability. The self-check, in principle, would test the function of each sensor element at intervals during normal operation with hardware incorporated in the sensor and controlled by on-board logic.

The periodic check must detect a failure in individual elements of the sensor, and also should identify the offending part so it can be quickly serviced or replaced. The functional check should be a quantitative, go-no-go type of test.

3.4.2 Redundant Design

The present sensor array has seven independent optical elements, each one of which has both a primary (8 meter) and secondary (2.5 meter) channel. Three of these elements are arranged with the illuminator beam at a height of approximately 1.2 meters. The remaining four beams are about 30 cm above the road surface. Lateral spacing of the elements is 15 cm. Therefore, conflicting traffic, which is expected to be pedestrians or cars, will be detected by at least two elements, so that failure of one element will not necessarily cause a system failure. However, a gap in the beam pattern will result, which will increase the probability that an unexpectedly narrow obstacle will be missed. The primary and secondary channels are independent, but overlap spatially. Therefore, an obstacle detected by one of them will cause the AMTV to slow, reducing the burden on the design of the backup bumper and contact switch.

It is recognized that a detailed fail-safe design of the electronic functions would be necessary to realize the full benefits of the redundancy inherent in the array sensor design (i.e., there is only one pulser for each half of the array). However, it is felt that the considerable and expensive effort required for such a design should come later in the development of the AMTV, after the basic design of all functions is well defined and not likely to change much. The focal plane array configuration described in Section 3-3 is significantly more redundant than the present design, and as a result, the performance degradation from a single failure will be less.

3.4.3 Checkout Techniques

Redundancy alone cannot ensure fail-safe operation, because, by design, the multiple channels will tend to obscure a failure. Some other procedure must be employed to detect any single failure before a second one occurs. Since failures are expected to be infrequent, daily checks performed as part of the routine for placing the AMTV in service may be frequent enough. Determination of the required frequency of the check-out would depend on the expected life-tme of the most critical components, and the specifics of the application.

Two types of checks can be performed: 1) a performance test of each sensor element using special test instruments, or 2) a functional test of the operating AMTV on a test target. The latter test was done on a regular basis during the earlier JPL AMTV experiment.

An example of an elementary performance test of the IR source would be a visual check with an IR viewer to see if all LED elements are lit. However, a quantitative measure of sensor performance, done element-by-element, is highly desirable. This measurement should not only check the operation of the complete opto-electronic channel, but should also measure the end-to-end gain and compare with predetermined limits. The way such a test might be mechanized for the focal plane array is indicated in Figure 3-7.

Each simulator element would be optically similar to its corresponding element on the AMTV. Thus, each LED or detector in the simulator would be coupled to the complementary element in the AMTV sensor. Sequencing logic would select each LED-detector element in order automatically, and correct function would be noted at the AMTV on-board controller. Signal thresholds and power outputs in the simulator would be carefully adjusted so that a minimum detectable return is simulated. Then, if a particular element were below a specified performance, the anomaly would be detected by the failure to deliver a sensor command to the AMTV controller.

Functionally, the AMTV could be driven up to the simulator, and the sequence completed in a few seconds with an overall pass-fail response. The associated logic could be programmed to read out which element was defective at the conclusion of the test.

The second type of test is a functional test of the operating AMTV. A test target would be placed in standardized positions on a

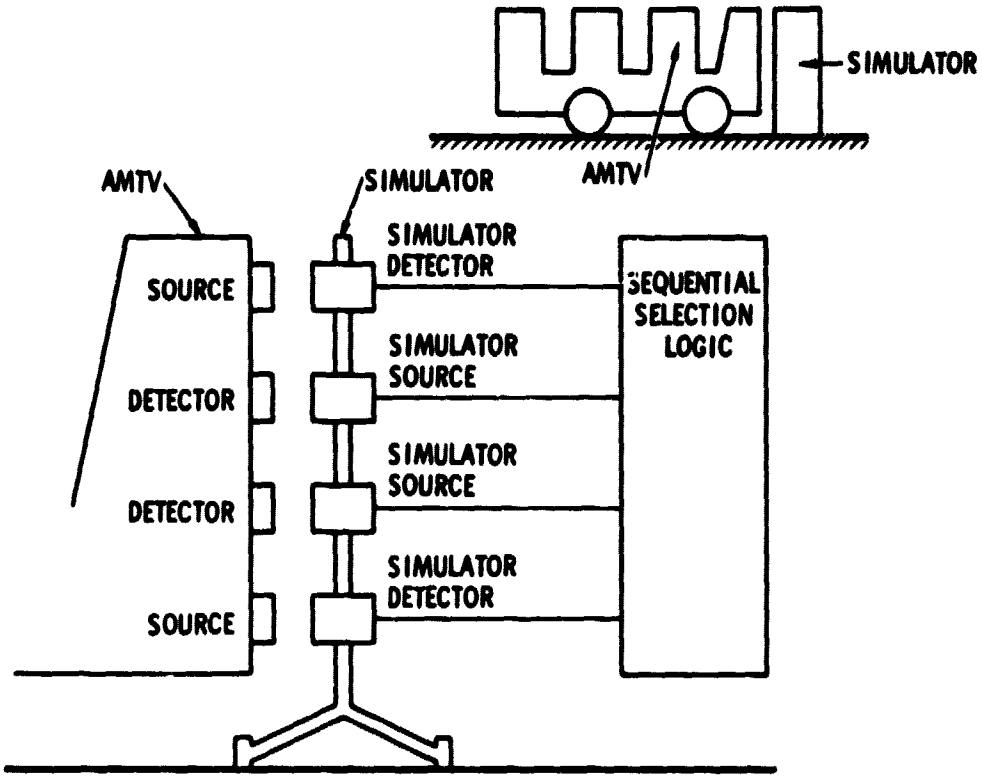

FIGURE 3-7. A CONCEPT FOR A HEADWAY SENSOR PERIODIC CHECK SYSTEM

test-track, and the distance remaining between AMTV and target after the vehicle stops would be measured. Change in this distance greater than a predetermined limit from check to check indicates service is required. Both this and the performance test just described could be implemented on a short piece of AMTV route guidewire in the service area as part of a daily, or more frequent, procedure. The procedure could be semi-automated, and would require only a minute or so per vehicle.

3.4.4 Self-Check Techniques

The check-out procedures just described could be performed in a similar way on the operating AMTV, if the necessary equipment were incorporated in the vehicle. A tradeoff exists between the cost and reliability of the added equipment on the one hand, and the frequency of the check on the other. The probability of an unsafe condition remaining undetected would, of course, be proportional to the test interval.

Introduction of an internal target or a calibrated light leak from LED to detector would provide the desired test, but mechanical elements must be used to switch the test on and off, and logic must also be provided to test each channel for proper function. The test target or the added monitors could be exercised each time the AMTV executed a timed stop. Another possibility would be to incorporate an additional detector in the sensor source optics to monitor light output, and an additional LED source to provide a test signal in each detector element.

SECTION 4

SENSOR ALTERNATIVES

In this section we discuss several alternatives for the headway sensing function. The types of sensor which are considered include the present optical proximity sensing array as a baseline for comparison, other forms of geometrical optical sensors, imaging sensors, laser range finders, ultrasonic sensors, and radar. We find that the proximity sensor array is able to meet the minimum requirements for a straight-ahead AMTV headway sensor as outlined in Reference 1-1. It is nevertheless important to examine other sensor types, which together with the rapid advances in electronic Large Scale Integration (LSI) technology, may make it possible to measure position and velocity of all potential obstacles, including those some distance to the side of the AMTV path and to exercise control based on such data. Development of such "smart" sensors is technically quite feasible now, but much too costly. Future technology advances may lower the cost and size of such systems to the point where they will be attractive for an AMTV.

4.1 OPTICAL PROXIMITY SENSOR ARRAY

The advantages of the present optical proximity sensor array are that it is simple (although the array has many elements to adjust), and would be relatively inexpensive to build. The definition of the sensed area is very good in the lateral direction ($\sim$15 cm). Although the desired longitudinal differential between black and retroreflective targets of 8-12 meters was not achieved for some of the array elements at worst case locations in the beam, the system functions satisfactorily on the road. The longitudinal resolution would easily meet the 8-12 meter differential with better quality lenses.

The focal plane array configuration described in the previous section is a possible future improvement in design that would simplify the overall installation, but it would operate on the same principle, and would have similar performance.

A drawback of the optical proximity sensor is that it is essentially a go-no-go type of device, which detects whether an obstacle is in the vehicle path. Only crude distance information is available from the primary-secondary channel separation. In order to obtain finer distance resolution, or to obtain lateral coverage for cruise turns and U-turns, the required number of sensor elements proliferates rapidly. One source-detector pair is needed for each bit of sensor information returned. However, integrated source arrays are possible, and integrated detector arrays(e.g., the CCD) already exist. Although practical considerations will probably preclude a "smart" sensor based on discrete source and detector components, the IC arrays together with appropriate techniques (Ref. 4-1) may well bear further study.

4.2 SCANNED LASER DETECTOR

A quite straightforward extension of the optical proximity sensor approach would be to replace the LED light source by a scanned laser. Proximity sensors of this type have been described in the literature. (Refs. 4-2, 4-3). Since noise from background sunlight is the limiting factor, the smaller spot size possible with a laser source would permit reduction in the detector field of view, and as a result would reduce the noise contribution from background light. With appropriate design, the resulting background noise reduction would permit the light source power or the response time to be reduced or the maximum sensing distance to be increased.

However, the complication of a mechanical scanner would be needed. On the whole, the advantage of using a scanned laser over the focal plane array proximity sensor configuration does not seem to be large. A detailed analysis would be needed to understand the tradeoff quantitatively.

4.3 IMAGING TECHNIQUES

Of significant interest for the headway sensing problem in the future are several techniques based on imaging sensors (TV cameras). A rudimentary experimental demonstration of vehicle control by imaging sensors has been conducted in Japan (Ref. 4-4), but it did not involve headway sensing. Although present-day vidicon cameras could be used on a vehicle like the AMTV, solid state cameras using CCD or CID detectors are under development and will probably continue to improve, both in reliability and in cost. The technology for electronic signal processing with Very Large Scale Integration (VLSI), which goes hand in hand with imaging sensors because of the very large amounts of data and the complex processing algorithms that are required, is also advancing at a very rapid pace. Progress in solid state imaging technology and VLSI should be watched carefully, because together they offer the promise of significantly more powerful headway sensing devices.

Stereo measurement from correlation of local areas in the images from the TV cameras is conceptually a simple approach, but its time has probably not quite arrived. The approach involves cross correlation to find the difference in position of the same feature in two images taken with cameras a known distance apart, and has been investigated in several laboratories. The computing requirements for correlation stereo of a real-world image in real time are formidable, and are beyond the present day state of the art, especially in a field instrument. Simplified images can be handled in a laboratory environment (Ref. 4-5). There is no basic reason, however, that the technique cannot become viable in the future with improvements in processing power.

4.4 LASER RANGE FINDER

Perhaps the most likely near-term approach for realizing a smart sensor is the laser range finder (LRF). The LRF is distinguished from the proximity sensor by the use of the propagation time of the light to the target and return to measure target distance. The tradeoff to determine whether the technology could be used on the AMTV is related to cost, not present technical

feasibility, and costs are decreasing. The ranging function requires nanosecond logic, but standard IC components which can do the job are available. An instrument based on a solid state injection laser is a good candidate for reasons of size and simplicity.

The literature on all types of laser ranging devices is too voluminous to discuss in this report, but the use of an injection laser for vehicular obstacle sensing was discussed by Kuriger (Ref. 4-6).

A scannable device for use in a robot system was described by Lewis and Johnston (Ref. 4-7) and a similar, but more refined instrument developed for a mapping application, has been reported recently by Mamon et al. (Ref. 4-8). Ranging accuracy within a half-meter or so and repeatability within centimeters has been obtained for timing of a single pulse and pulse repetition rates could be 10^4 to 10^5 sec^{-1}, adequate for area coverage in real time.

A mechanical scanner would be necessary to cover an area with one laser (or possibly a few), because of the cost of the lasers ($200-$300 each). The power required from the source is larger than necessary for a proximity sensor because the detector channel bandwidth must be compatible with nanosecond timing, but the average power emitted from the source optics is still in the milliwatt range, and, according to Mamon, the instrument is eye-safe (Ref. 4-8).

A sketch showing conceptually the application of an LRF to AMTV headway sensing is shown in Figure 4-1. A single instrument mounted on the canopy would scan the area in front of the vehicle. Unlike the case of the present proximity sensor, three-dimensional coverage to the full height of the vehicle would result. Additionally, the road surface would be detected continuously, providing a fail-safe check of sensor function.

The LRF can be a smart sensor in the sense that an area considerably wider than the vehicle can be covered, so that turns can be handled and potential collisions with crossing traffic can be anticipated. The processing needed to work with data in a three dimensional map, and to implement a more general control law based on it is of the type that the mainstream of microprocessor technology can handle.

4.5 ULTRASONIC SENSING

Ultrasonic detection has been widely applied, and the small size and simplicity of such devices are very attractive for the AMTV application. In an ultrasonic sensor, the sonic wave is generated by a ceramic transducer which is typically a plane wafer emitting in a direction normal to its surface. The echo is detected by the same transducer.

For the purpose of evaluating ultrasonic sensing, a Polaroid Pronto camera was purchased. The sonic ranging elements were removed and interfaced with conventional digital electronics to display range in meters or feet. The basic hardware is described in further detail in Appendix D, along with some laboratory test results obtained with it.

In principle, the triangulation scheme just described could yield location of obstacles within an area. However, a distributed target such as a row of parked cars alongside the AMTV path could not be handled by simple triangulation, and therefore, as is, the scheme will not satisfy the AMTV requirements. If suitable processing could be devised to handle a distributed target, ultrasonic triangulation would make a very attractive AMTV sensor. For example, phased transducer arrays have been used to return image-type data (Ref. 4-9).

4.6 RADAR

Microwave radar shares several characteristics with the ultrasonic sensor, having a broad beam but yielding accurate distance or velocity data directly. Modern microwave technology can provice a small, relatively inexpensive instrument, as seen in highway speed radar devices. Compact radars have been used for aircraft terrain clearance sensors, train speed determination, and other industrial uses. The use of radar has also been studied as a possible sensor for prevention of automobile rear-end collisions (Ref. 4-10).

Although the radar instrument proper can be compact, the beam spread with an antenna of reasonable size will be many degrees wide. The discussion of triangulation techniques for ultrasonic sensing is equally applicable here, and the problem of dealing with an extended object is the same. In order to achieve the required lateral definition (15 cm at 8 meters) directly, the overall antenna size would have to be of the order of the frontal area of the AMTV, too large for a steerable antenna, but perhaps feasible for a phased array.

For the present, it is felt that radar cannot be ruled out as a future AMTV sensor, but the complication of providing a suitable antenna would make such a sensor difficult to implement.

SECTION 5

AMTV BODY DESIGN FOR SAFETY

In this section, the results from a study of vehicle safety design for the AMTV are first discussed, and possible AMTV body concepts based on the safety study are presented. Finally, a few design sketches indicate to the reader what a future AMTV might look like. Attention was focused on three different areas - an investigation of contact switch sensors, a study of energy absorbing bumpers, and the development of AMTV body design concepts.

The basic requirements addressed were to eliminate or minimize the potential for injury to pedestrians in vehicle-pedestrian impacts at a nominal vehicle speed of 11 kph and a maximum vehicle speed of 24 kph, and to minimize the chance of injury to passengers in the event of a collision with another vehicle or obstacle at the same speeds. While the primary and secondary headway sensing system should minimize the possibility for such impacts to occur in the first place, it is very desirable to apply a high reliability and fail-safe design approach, including redundancy in critical areas. Final decisions on the pedestrian and occupant protection design options discussed below should be made with due consideration of the overall level of redundancy felt necessary and practical for the specific AMTV application.

In general, the suggested impact attenuation provisions presented below are conservative. They assume that the following potential hazards must be considered:

(1) Pedestrians are impacted by the AMTV front at closing velocities up to 24 kph.

(2) Collisions with other vehicles or obstacles occur at closing velocities up to 24 kph.

(3) Objects overhanging the AMTV route (e.g., tree limbs, signs, and lumber on trucks) are somehow missed by the optical sensors.

(4) AMTV users or other pedestrians stand too close to the side of the vehicle while waiting for the vehicle to move out of their path.

In the present 3 to 11 kph, prototype AMTV a contact bumper-switch (i.e., a "cats whisker") was provided to sense an impending pedestrian-vehicle front impact and apply the vehicle brakes. In the next generation of AMTV's, it is felt that a similar contact sensor (or at least the function provided by the current cats-whisker) should be maintained.

5.1 CONTACT SENSING SWITCHES

A number of potential candidates were identified by various means, as follows:

- o Cats whisker with microswitch in beam mode (i.e., the present device).
- o Articulated cats-whisker with microswitch in deflection sensing mode (this is illustrated in a subsequent section of this report).
- o Ribbon switch (e.g., steering wheel rim horn switch, gate or door openers).
- o Trip cord (e.g., bus stop signal cord).
- o Pneumatic or hydraulic hose type devices (e.g., service stations).
- o Elastomeric strain gages.
- o Air or fluid pressure in a pneumatic or fluid bumper.

Other sensing candidates identified included non-contacting sensors such as a tertiary headway sensor of the optical type, radar, sonar, capacitance, etc. Non-contacting sensors were not considered seriously because it is a common practice to make the final or fallback safety system as simple and as reliable a mechanical or electrical device as possible. Criteria selected for narrowing the number of sensing candidates include:

- o Compatibility with pedestrians (e.g., minimal abrasion, snagging, tripping or motion interference).
- o Compatibility with the energy absorption bumper configuration selected.
- o Reliability and simplicity.
- o Applicability to large areas of the vehicle (including sides, rear, and vision areas).
- o Reaction time constant.
- o Capacity for auto-reset.
- o Susceptibility to vandalism.
- o Initial service and replacement costs.

Based on a largely subjective review of the above, the candidate contact sensors suggested for use in the next generation AMTV's are the articulated cats whisker for an "advance warning" of an impending pedestrian/vehicle contact and a ribbon type switch for actual contact between the vehicle and a pedestrian or other obstacle. The articulated cats-whisker is suggested over the present non-articulated form for two reasons - (1) it should pose less of a tripping or entrapment hazard and (2) it can be stowed readily to facilitate driving the vehicle over sharply angled ramps.

The ribbon type switch (see Figure 5-1) is favored over some of the more complex switch/sensor forms because of its commercial availability, light (as low as 225 grams) contact pressure requirements, likely durability, fast response time, and likely low cost. Several firms are listed in the Thomas Register which are potential sources of this device (two of these firms are Tapeswitch Corporation of America, Farmingdale, N.Y.; and United Security Products, Inc., Dublin, California.)* These particular devices are typically used for safety purposes on the edges of power actuated doors and moving machine elements. Some of them also provide a padding function as well as a switch function. It is anticipated that these ribbon switches could be adhesively mounted to any desired location. At the outset it seems desirable to mount them to the leading edge of the front bumper, the entire periphery of the roof or canopy, and selected body side surfaces which would sense contact of pedestrians too close to the vehicle sides or obstacles contacted during sharp turns.

One of the concept vehicles presented below features the use of a safety net as an impact attenuation device. A contact closure could also be obtained from such a net by attaching a trip cord or microswitch sensor to sense any significant deflection or tension changes in the net.

Another device which might be considered for any of the concept vehicles described is an override sensor to detect any obstacles which may be missed by the cats-whisker. This function might be provided by a hinged, thick rubber curtain hanging from the leading edge of the vehicle's

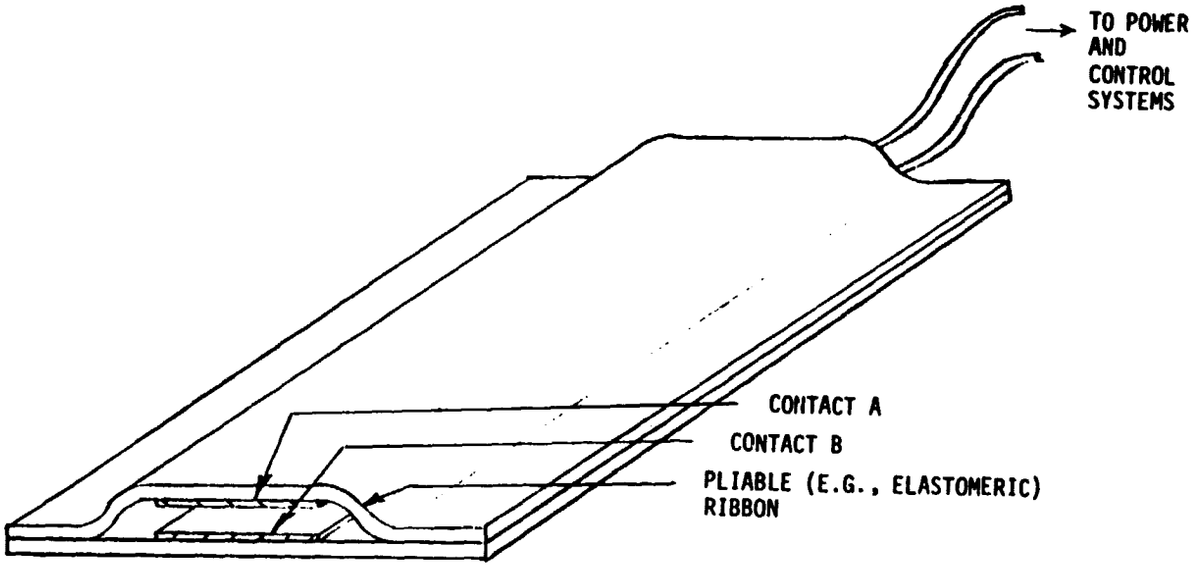

FIGURE 5-1. SKETCH OF RIBBON SWITCH CROSS SECTION

*Potential sources identified here and elsewhere in this report are not necessarily the best or only sources which should be considered. They are listed here only to serve as examples or starting points for subsequent procurement activity.

undercarriage and running its full width. Significant tilting of this curtain or flap could be detected by a trip cord, mercury switch, string potentiometer or other motion sensing device. A precaution with this and some of the other sensing devices is to ensure that excessive numbers of false alarms do not occur.

Use of pneumatic and hydraulic type pressure sensors might also be viable in certain AMTV applications. However, these types of devices were not favored in this initial screening effort because of their relative complexity and some concern about their long-term durability and response times.

5.2 ENERGY ABSORBING BUMPERS

For purposes of this study, the term "bumper" is interpreted to mean the entire front structure of the AMTV as opposed to just the typical automotive bumper. Based on previous work at Battelle (Ref. 5-1, 5-2, 5-3, 5-4), it is known that impact event trajectories can be estimated based on initial pedestrian-vehicle geometries and the impact velocity. In general, for the impact velocities anticipated for the AMTV's, it can be expected that an impacted pedestrian will pivot into the front of the vehicle by rotating about the point of initial contact (e.g., knee, thigh, or hip). Because the present and proposed AMTV fronts are likely to be fairly blunt and only 1.8 meters tall, protection against potential pedestrian head impacts must be provided over much of the remainder of the front surface to accommodate a wide range of adult and child pedestrians.

A variety of human injury criteria have been used in the literature for the different body sectors. For initial design purposes, an allowable peak g criterion is often used. Values of this type thought to be appropriate for the AMTV application are as follows:

Head - 80 g, 3 ms duration
Chest - 60 g, 3 ms duration
Pelvis - 40 g
Knee/leg - 80 g

It should be noted that the head and chest values shown represent survivability limits and that the pelvis and knee/leg values correspond to injury threshold values. Therefore, the design head and chest values should be kept as far below the tolerance values shown as possible for both the pedestrians and the vehicle occupants. The pelvis, knee and leg values, however, could be allowed to approach the tolerance values indicated.

Expected peak deceleration values for several selected cushioned impacts at the AMTV's design speeds are shown in Table 5-1. Other scenarios were briefly investigated involving pedestrians walking or running into the AMTV at various individual velocities. While some of these other scenarios would yield closing velocities greater than 24 kph, their probability seems low. It was decided, therefore, to focus the initial design work on a 24-kph closing velocity, but to leave some margin of safety to accommodate the more stringent scenarios. It should be noted that it is usually not possible to achieve uniform deceleration rates with practical, passive, energy absorbing structures. Therefore, for initial design work, it should be assumed that the

TABLE 5-1. ANTICIPATED PEAK DECELERATION* (G's) AS A FUNCTION OF CUSHIONED STOPPING DISTANCE AND CLOSING VELOCITY

Closing Velocity	Padding Thickness (cm)					
	5	15	20	25	30	45
24 kph	90	30	24	18	15	10
11 kph	17.8	6.6	5.4	4	3.2	2.2

*These peak deceleration values are double the values that would be expected at constant deceleration.

actual peak values generated will be approximately double those predicted for uniform deceleration, because the anticipated deceleration time waveforms will be bellshaped curves instead of square waves. In consideration of these various factors, it was decided to provide 20 cm of bumper compliance in likely pelvis impact regions, and 15 cm in likely head, chest, and knee/leg impact regions of the AMTV front. Other possible impact surfaces (e.g., in the vicinity of the headway sensors or hard spots in the vehicle interior) should receive a minimum of approximately 6 cm of impact cushioning.

Several ways of embodying these cushioning requirements into next generation AMTV's are presented in the next section of this report (5.3).

In regard to the "bumper bar" element itself, however, one further point should be noted: AMTV bumper design involves a tradeoff between pedestrian protection, occupant protection, and vehicle damageability. For the sake of pedestrian protection, the bumper should be quite soft and low enough to strike near the center of the long bones of the lower leg. From the standpoint of occupant protection, the bumper system should have a long stroke but usually a much stiffer compliance rate than that desired for optimal pedestrian protection. Finally, from the standpoint of both occupant protection and vehicle damageability, the height of the AMTV bumper bar from the ground should match the standard bumper height of the cars with which it may collide. As will be shown shortly, the suggested compromise is a hybrid bumper bar featuring (1) a soft front edge for pedestrian protection, (2) a stiff reinforcement beam mounted on two hydraulic energy absorbers for occupant protection and damageability, and (3) an AMTV bumper bar height which matches U.S. passenger cars to ensure effective bumper system performance in potential car/AMTV collisions.

One further front structure consideration involving some compromise concerns the presence and nature of a windshield. The laminated windshields in U.S. passenger cars are an effective occupant restraint device in that they keep the occupants inside the vehicle in the event of a crash. They are not, however, as non-injurious an impact site as say a padded dash for either the occupants or the pedestrians. The "windshield" area options for the AMTV application include (1) a padded wall in place of the typical windshield opening, (2) a windshield opening with no glazing, (3) a windshield opening

with a see-through net in place of normal glazing, (4) a normal glazing of automotive safety glass, (5) a quasi-pliable polycarbonate or acrylic plastic glazing, (6) some hybrid of the above. Considering (1) that the data for occupant and pedestrian head/safety glass impacts (Refs. 5-5, 5-6) at 24 kph are significantly less than the nominally accepted head injury criteria value, (2) likely long-term durability, and (3) likely user reaction - the compromise suggested is to use automotive safety glass mounted in accordance with present automotive practice.

5.3 DESIGN CONCEPTS

Once guidelines had been established for the sensing and impact attenuation devices, a number of concepts were sketched to identify potentially viable combinations and options. It was found that the variations could be grouped into three categories: (1) an open bodied design very similar to the present tram and (2) a custom semi-enclosed design of the same approximate size as the present tram. It was anticipated that features of these various engineering oriented concepts could be hybridized with each other or with features embodied in the nicely stylized concepts done by David Robb.

5.3.1 Front Treatment

A sketch showing a suggested treatment of the AMTV front-end design is shown in Figure 5-2. A cutaway section is used to show the relationship of the added energy-absorbing padding to the front structure of the AMTV, and to human figures drawn to the same scale.

Pedestrian impact protection is provided primarily by four horizontal "bumpers" of relatively soft (e.g., approximately 48 to 64 kg per cubic meter density) foam. The foam would be open celled (for energy absorption) polyurethane covered with a tough polyurethane skin or glove for durability. Some coring of the foam from the unskinned side or edges may be required to optimize the final compliance of the bumper assembly. This coring operation (i.e., provision of slots or holes) is performed after the bumper is molded and prior to its final installation on the vehicle. A layer of the same foam (6-cm minimum) would be applied across the front face area in the vicinity of the headway sensors and on any likely hard spot impact points in the vehicle interior. Potential sources for foam bumpers/fascias include the Davidson Rubber Co., Dover, New Hampshire; and the Bailey Division, USM, Seabrook, New Hampshire.

It should be noted that selection of an impact attenuating material and design approach for the AMTV front involves a number of tradeoffs: (1) softness for impact attenuation versus stiffness for durability; (2) broad coverage versus non-interference with the headway sensor lenses and forward visibility for the occupants; and (3) pedestrian protection versus occupant protection. For example, very soft foams may not be sufficiently durable, but moderate to stiff foams may not yield the desired cushioned stopping distances unless the bumpers are formed with very narrow cross sections in the direction of deflection. As another example, the

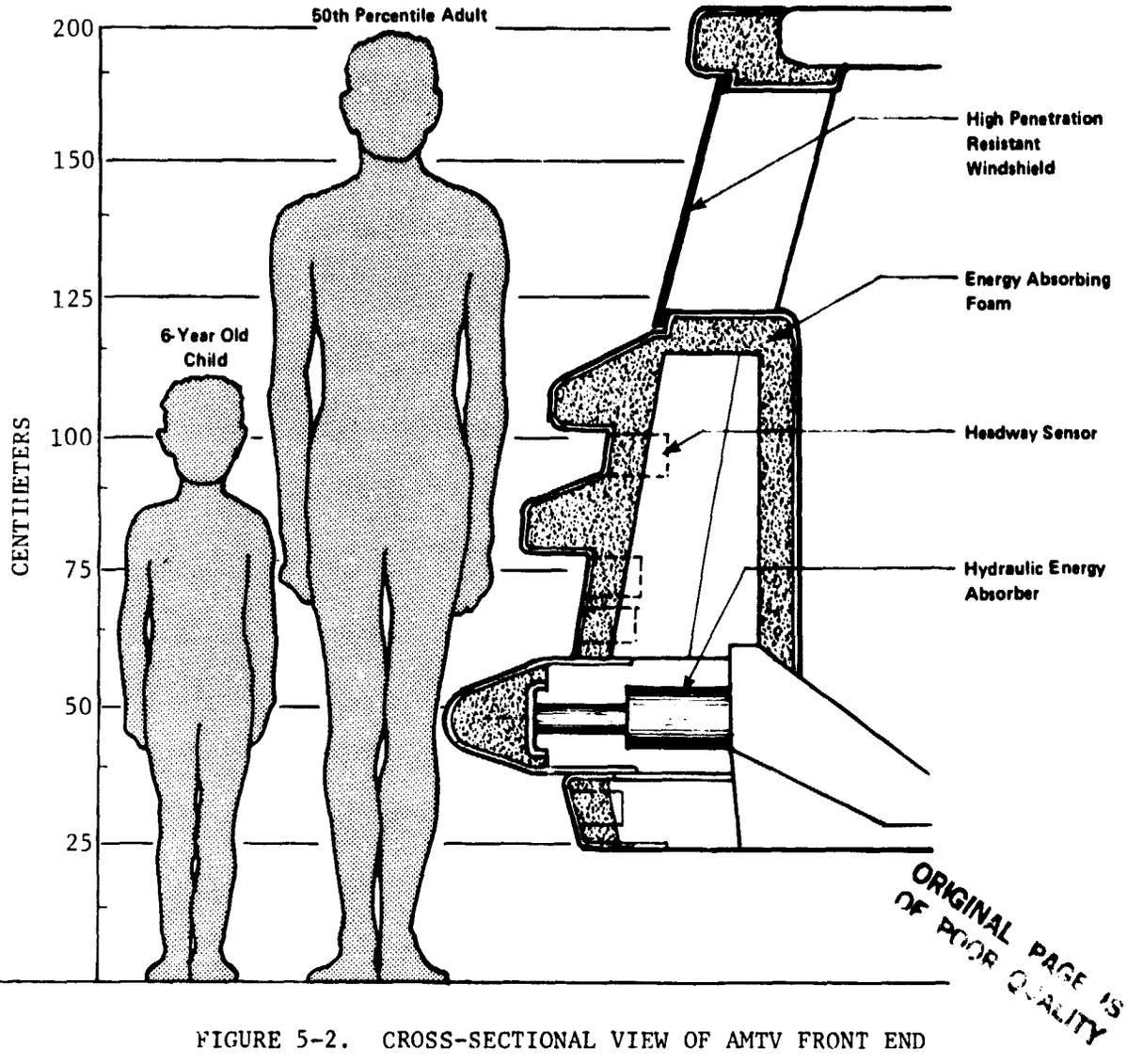

FIGURE 5-2. CROSS-SECTIONAL VIEW OF AMTV FRONT END

windshield area could be glazed with a pliable, lightly mounted plastic window or left open as in the present tram. While either of these windshield approaches might satisfy the pedestrian protection requirements, they may not provide the desired occupant protection against (1) intrusion by overhanging signs, lumber protruding from the back of a truck, etc. or (2) occupant ejection in a frontal collision. For this particular hazard combination, a protective net or automotive safety glass is preferable.

Also included in Figure 5-2 is a structurally stiff steel or aluminum bumper bar reinforcement embedded in or backing up the lower 15-cm foam pedestrian impact bumper. This structural bumper would be mounted on 15-cm stroke hydraulic or viscoelastic energy absorbers similar to those used on present U.S. produced automobiles. Possible sources for these energy absorbers include the Menasco Automotive Products Division, Burbank, California and the Delco Division, GMC, Dayton, Ohio. The purpose of this structural bumper and energy absorber system would be to (1) attenuate vehicle acceleration forces which the vehicle occupants will be exposed to in the

event of an accidental collision with another vehicle or a rigid obstacle and (2) minimize accidental damage to the AMTV itself.

5.3.2 Occupant Protection Concepts

Features which could be incorporated into an AMTV design in order to provide added protection for occupants are illustrated in the sketch, Figure 5-3. The safety items include:

(1) An energy absorbing net on the vehicle front to minimize the likelihood of pedestrian contact with the frontal areas between the soft bumpers. This netting would also (a) afford something for a struck/falling pedestrian to grab onto, (b) prevent a struck pedestrian from intruding into the occupant compartment and possible injuring himself or an occupant, and (c) provide (via trip cord sensors attached to the net) both an additional means of sensing pedestrian contact and a positive means of sensing overhanging signs, tree limbs, lumber protruding from a truck, etc.

(2) Provision of energy absorbing nets (or high seat backs) to prevent (a) occupant whiplash in the event of a rear-end collision and (b) unrestrained forward motion of the occupants in the event of a front-end collision.

(3) Stronger side columns to minimize intrusion and occupant injury in the event of a side collision.

FIGURE 5-3. OCCUPANT PROTECTION FEATURES

5.3.3 Open Tram Design

A suggested design for an open tram is shown in Figure 5-4. As indicated above, this concept is intended to represent what might be done in the way of a minimum change from the present tram. It is suggested that contact sensing (in addition to the cats-whisker bumper switch) for the AMTV front, rear, or side surfaces be provided by ribbon strip switches.

FIGURE 5-4. AN OPEN TRAM DESIGN CONCEPT

Not shown in the figures, but recommended for all of the design concepts, would be "curb feeler" types of devices located near the ground level immediately in front of each of the wheels. These devices would sense the presence of a careless pedestrian's feet, trigger a characteristic alarm, and prevent the vehicle from moving until the endangered foot is moved out of the way. Use of large clearance wheel guards and/or soft flotation tires would be other means of minimizing this hazard.

5.3.4 Enclosed Tram Design

A possible semi-enclosed configuration is shown in Figure 5-5. In this figure the safety design concepts discussed above were combined by an artist with styling ideas to show the overall appearance an AMTV might present. While retaining the basic size of the present tram, this concept represents an attempt to provide a highly enclosed design which could be adopted for improved safety and potential compatibility with all-weather operation. In addition to improved structural integrity and occupant protection in front, side, rear, or rollover collisions, if properly constructed, doors could provide additional occupant protection in the event of side collisions. Furthermore, with the use of door closure sensors, and safety interlocks in the control logic, additional benefit should be obtained with regard to reducing potential boarding hazards.

In Figure 5-6, another artist's rendition is shown of an open AMTV, but using a different front treatment. In this sketch, a smoothly styled front surface is shown, rather than the padded ridges for energy absorption. This could be done with appropriate hollowing out of the smooth padding in order to achieve the desired compliance.

Figures 5-7 and 5-8 call out some of the features shown in the sketches, and Figure 5-9 indicates a concept for package carrying.

5.4 CONSIDERATIONS FOR FUTURE ACTION

Finalizing the design of the next generation AMTV will involve a number of factors, for example, detailed analysis of the specific mission and payload requirements, operating environments, selection of the basic vehicle chassis to be used, establishment of prototype design and development time and cost constraints, and formulation and execution of a vehicle build and development plan. The configuration presented in Figure 5-5 represents the currently favored choice of the project team. However, depending on the exact requirements of the specific application for the next generation AMTV, any of the other concepts or combinations of them may be viable candidates.

The primary considerations for future action identified by this study all revolve around optimizing the selection of pedestrian (and occupant) safety measures. A possible starting point for such an optimization effort would be to review/update the Failure Modes and Effects Analysis in Reference 1-1 to reflect (1) any new AMTV capabilities provided by currently foreseen changes in the headway sensors, control logic, and pedestrian/occupant safety measures and (2) a reassessment of the criticality or risk of any of the

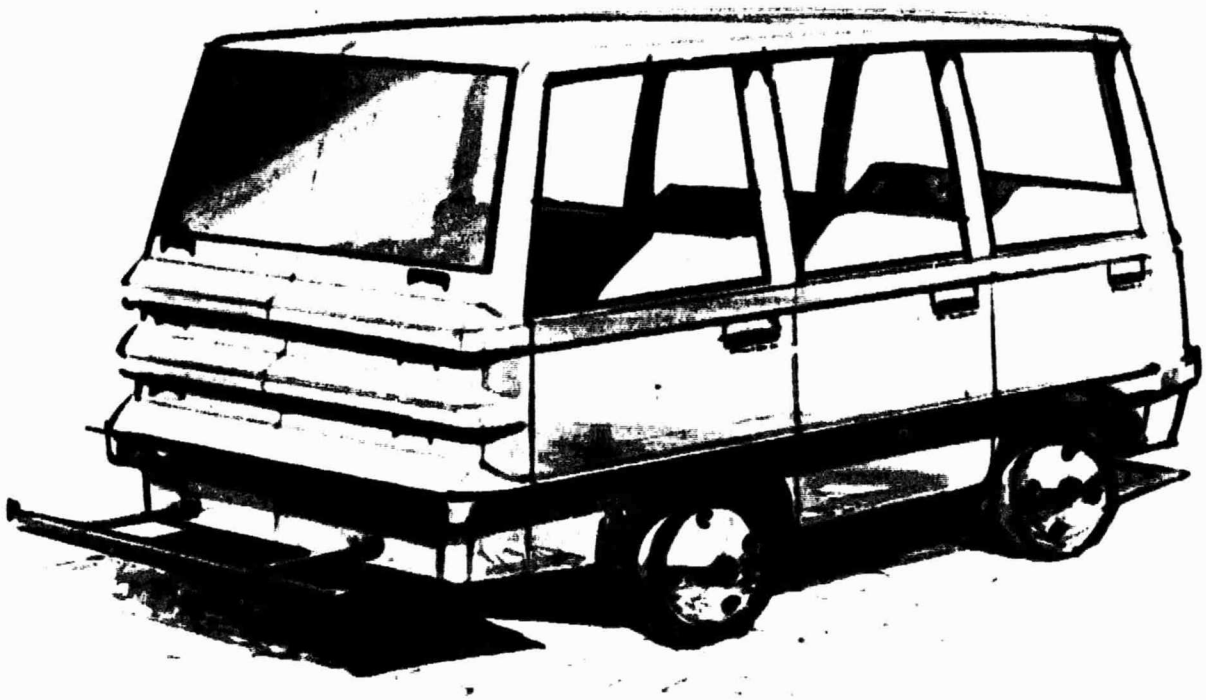

FIGURE 5-5. ARTIST'S CONCEPT OF A SEMI-ENCLOSED AMTV BODY DESIGN

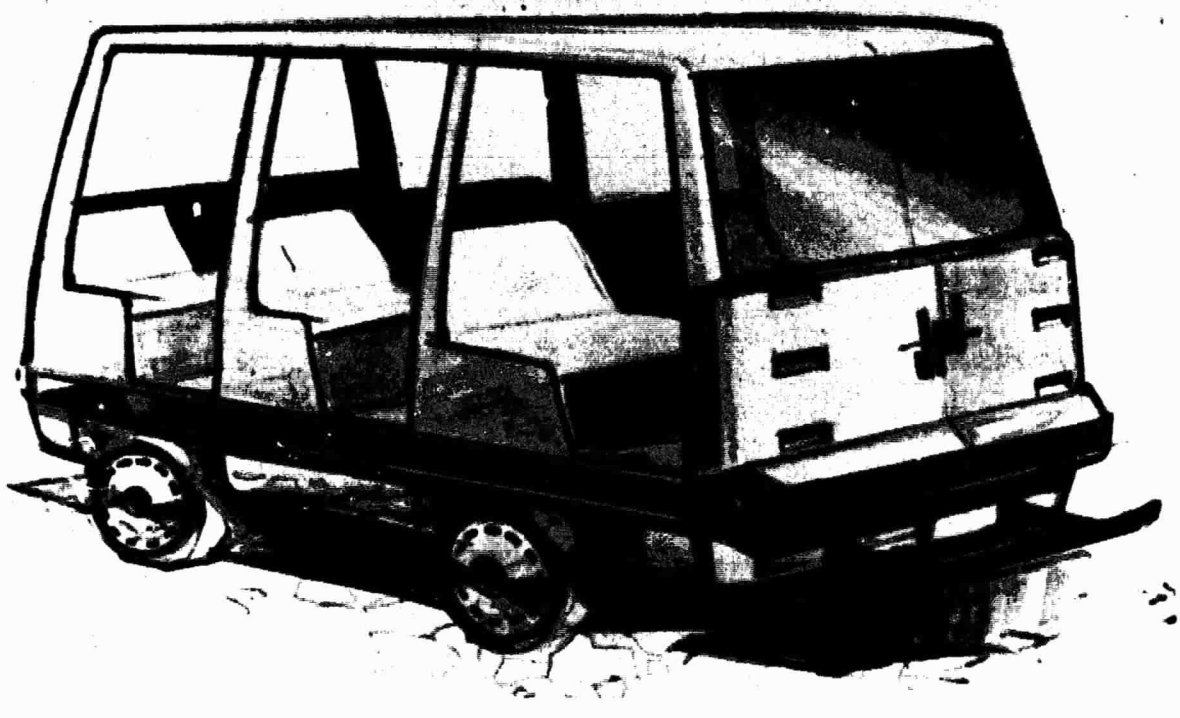

FIGURE 5-6. ARTIST'S CONCEPT OF AN OPEN AMTV WITH A SMOOTH FRONT TREATMENT

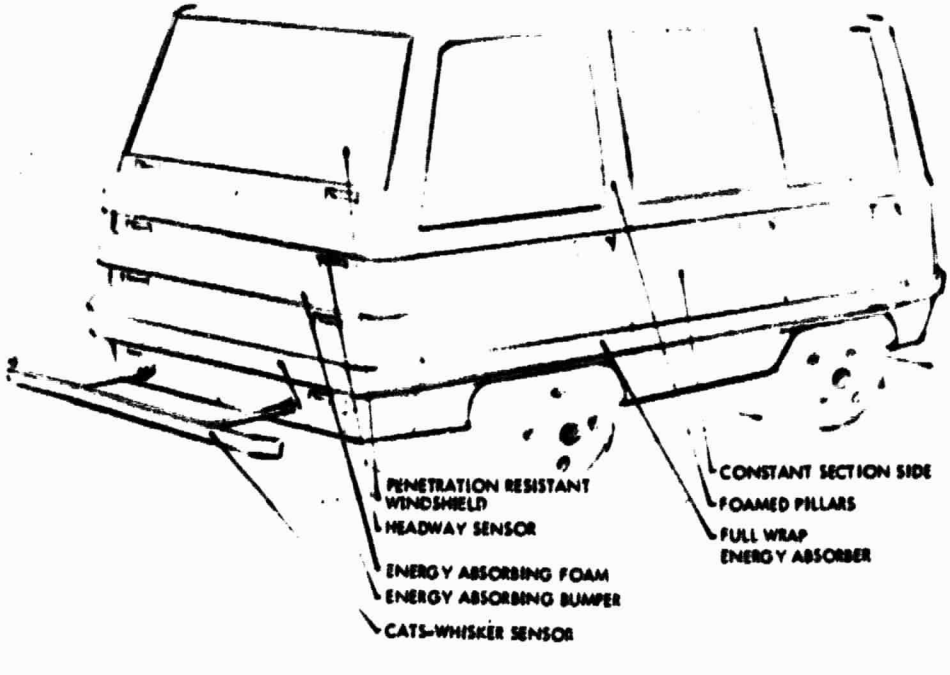

FIGURE 5-7. SKETCH IDENTIFYING FEATURES SHOWN IN FIGURE 5-5

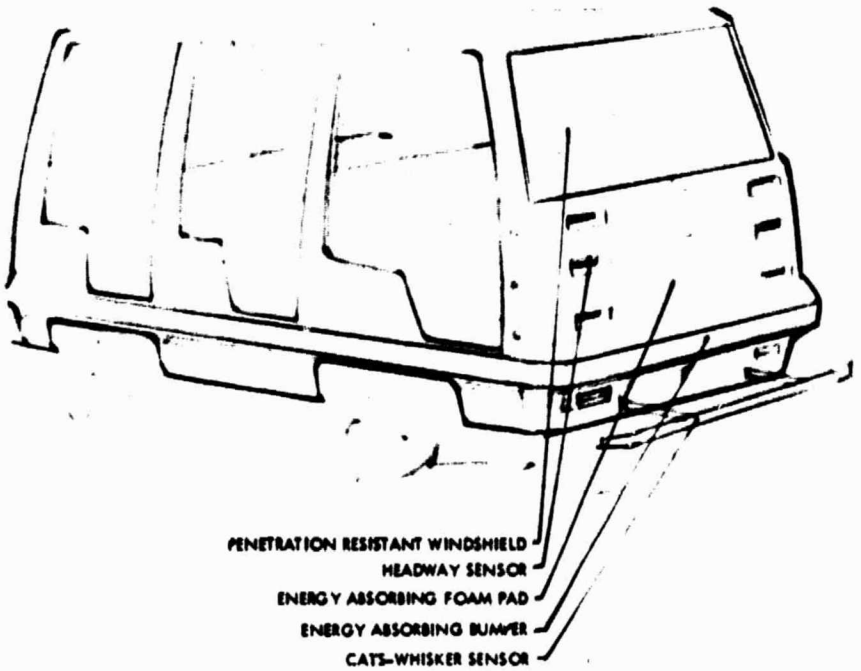

FIGURE 5-8. SKETCH IDENTIFYING FEATURES SHOWN IN FIGURE 5-6

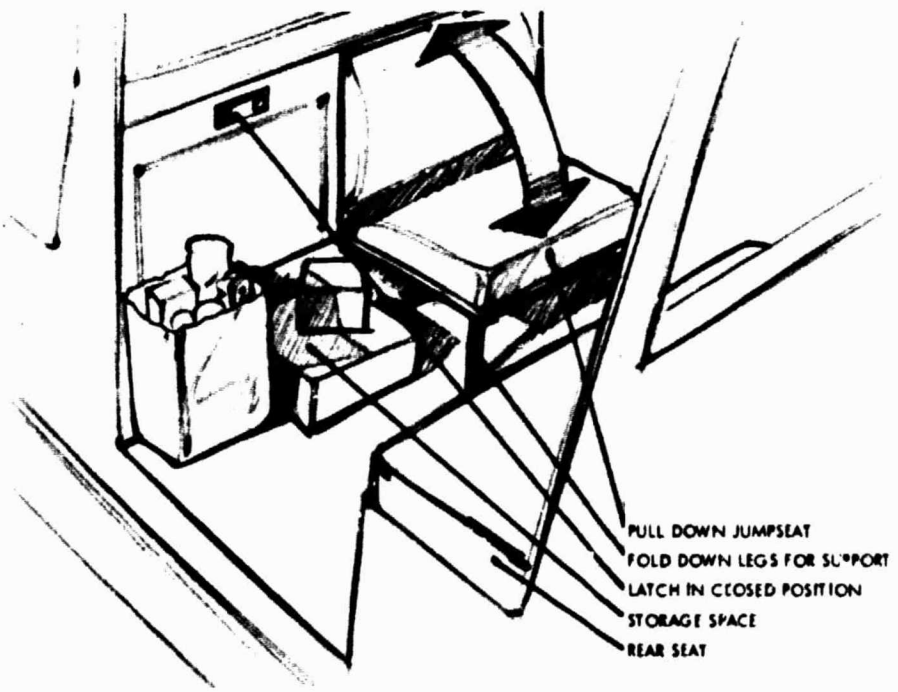

FIGURE 5-9. A CONCEPT FOR PACKAGE CARRYING ON AN AMTV

possible failure modes based on (a) the currently foreseen changes in the AMTV and (b) the specific demands likely to be imposed by the actual application selected for demonstrating the next generation AMTV. A possible outcome of such an effort might be a decision to modify the control logic to enhance occupant safety by taking advantage of the available pedestrian impact protection features and allowing a slightly less stringent deceleration rate when the cats-whisker pedestrian sensor encounters a pedestrian or other obstacle. Other possible outcomes might be to (1) confirm a need for contact sensors on the sides of the AMTV but not the rear, (2) require further upgrading of the occupant protection features for anticipated side collisions by other vehicles, (3) dictate a need for evaluating the selected pedestrian or occupant safety measures in full scale crash tests, etc. As with nearly any safety study, the number of contingencies is almost limitless. It is, therefore, likely to be impractical to develop, demonstrate, and provide many more countermeasures than those demanded by the normal use and anticipated misuse conditions posed by the specific intended application.

APPENDIX A

AMTV ARRAY SENSOR DESIGN

DESCRIPTION AND CIRCUITS

The array sensor is made up of seven elements, each consisting of an LED illuminator unit, a primary detector and a secondary detector as seen in the photograph in Figure A-1. In Figure A-2 elements 1, 2, 3 and 4 (the lower sensors) have an operating frequency of ~1000 Hz and 5, 6, 7 (upper sensors) operate at ~1100 Hz. The two frequencies are required to prevent the lower primary detectors from seeing the road which is illuminated by the upper LED units. Each of the above elements is aimed straight ahead. Elements 8 and 9 are used only while turning and are aimed at an angle to the side (see Appendix B). Figure A-3 is a block diagram of the array sensor system. The system has the following parts:

(1) Dual Frequency Pulser. A dual voltage multivibrator (VCM) generates the two frequencies, ~1000 Hz for the upper sensors, and ~1100 Hz for the lower sensors. These signals are amplified, drive the LEDs through current limiting resistors and also supply the reference signals for phase sensitive demodulators in the amplifier-demodulator cards.

(2) Optical Units. The optics are identical for the LED light source and the detectors (Figures A-4 and A-5). They have a 75 mm focal length and a 5 cm diameter which is stopped down to 3.2 cm and the housing is provided with four baffles. An integrated detector/amplifier* is used in the detector units. Each detector has an optical filter which passes the IR signal and attenuates visible light.** The voltage outputs are summed in the amplifier-demodulator cards.

(3) Amplifier-Demodulator Card. There are four amplifier-demodulator cards, as shown in Figure A-3. The primary and secondary cards are identical except for an appropriate gain adjustment. A 0.1 second RC filter couples the output of the demodulator to a threshold level detector, which has a digital output. The threshold level detector has a small amount of hysteresis to prevent switching due to noise when the signal level is near the threshold level.

(4) Logic Card. The two logic blocks in Figure A-3, one for the primary signals, and the other for the secondary signals, combine their inputs to form a logical OR output. The primary card output is the SLOW signal and the secondary card output is the STOP signal.

*Bell & Howell 529-2-5 integrated optical detector.
**Kodak wratten filter No. 87C.

SENSOR PERFORMANCE

Two targets were used to take data (Figure A-6), a black target, 120 cm high painted with black paint having a reflectivity of 0.5% at 0.9μ*, and a retroreflector target made up of ten 11.4 x 4.8 cm reflectors. The black target was always used in the vertical position, while the retroreflector target was in the horizontal position for determining the vertical profile of the sensor beam and in the vertical position for the horizontal profile. The sensors were first adjusted so that the LED and primary beams converged at 5 meters, and the LED and secondary beams converged at 1.5 meters. This was done by placing an IR source (LED) at the center of the projected image of the LED optical unit, as observed with an IR viewer at the desired distance (1.5 meters for the secondary and 5 meters for the primary detector) from the array sensor. The detector optical unit was then pointed for maximum output from the amplifier-demodulator card. Figure A-7 shows the outline of the sensed area, using the black target, for the sensor array when it was adjusted as described above. The figures are plots, to scale, of the measured sensor threshold, viewed from above. Inside the plotted boundary, the sensor system would indicate an obstacle present; outside, it would indicate clear. Errors in pointing individual elements result in an irregular cutoff.

In order to obtain a more uniform cutoff distance, as desired, the same tests were repeated following a different adjustment procedure. In this case, each individual detector unit pointing adjustment was made such that the threshold was just reached for the black target at the desired distance.

In effect, the adjustment tailored the black target response to cut off at a uniform distance, as shown in Figure A-8. The threshold response for the retroreflector target after the sensors were adjusted in this way is also shown in Figure A-8. The data points shown are seen to follow a pattern alternating between longer and shorter distance. The more distant data points are when the retroreflector is in line with the sensor element axis, while the points midway between are when the retroreflector is midway between the sensor axes (the width of the retroreflector target is 11 cm and the sensor spacing is 16 cm). Four of the sensor elements detected the retroreflector target beyond 30 meters, while the others were 11 meters or less. The reason for the longer than desired cutoff distance is primarily the imaging quality of the single-element lenses used in both LED and detector units. The on-street performance of the array sensor system, as it is, appears to be satisfactory in spite of the over-long cutoff for a retroreflector. Selection of higher-quality lens would eliminate the problem. With some fine tuning the sensor output could have been made more uniform, but this was not felt to be important enough to be justified at this time.

Figure A-9 shows the location of the threshold of a single primary sensor for the retroreflector target in the horizontal position as a function of the vertical position of the target. Figure A-10 shows the threshold distance as a function of lateral target position, for the same sensor set (retroreflector in vertical position). Similarly, the response of a single sensor set as a function of target distance for the black target, showing the threshold levels and the saturation levels are shown in Figure A-11 (primary), and Figure A-12 (secondary).

*3M Company Nextel Velvet Coating 101-C10 black.

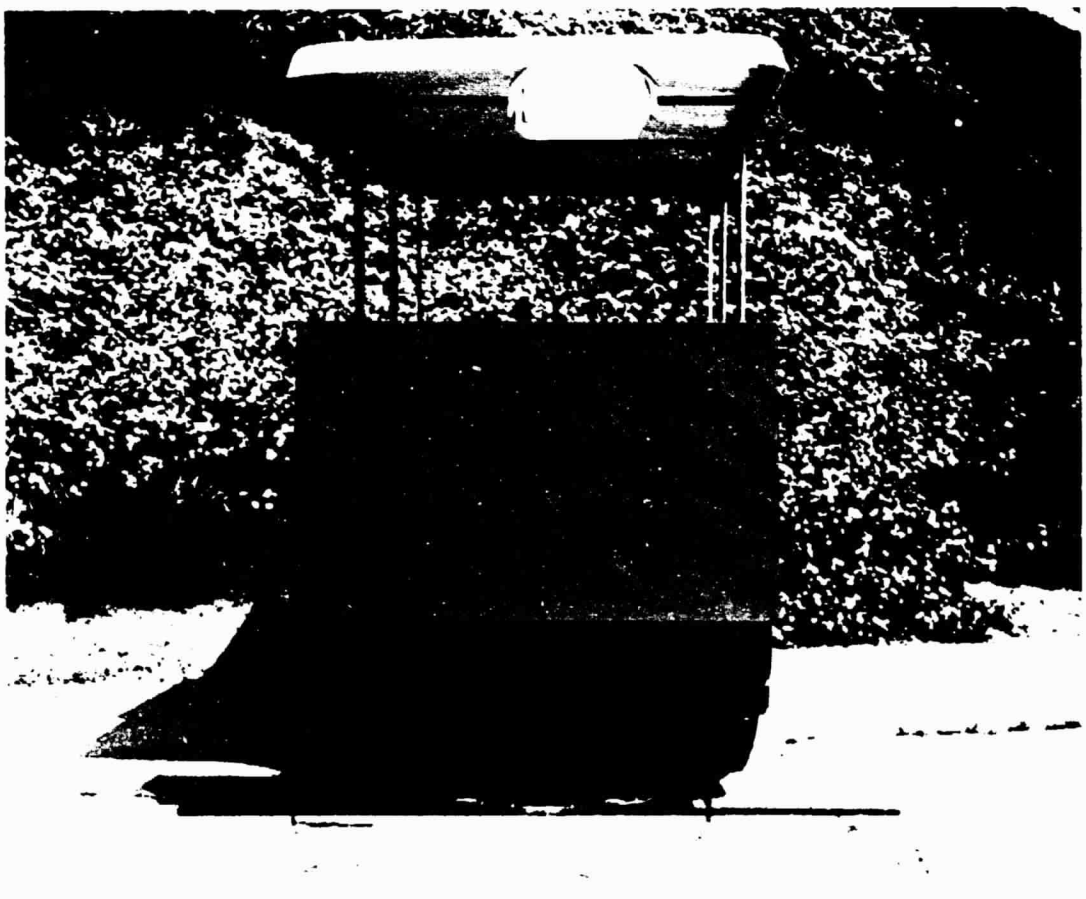

FIGURE A-1. OPTICAL PROXIMITY SENSOR ARRAY INCORPORATED IN THE PRESENT JPL AMTV

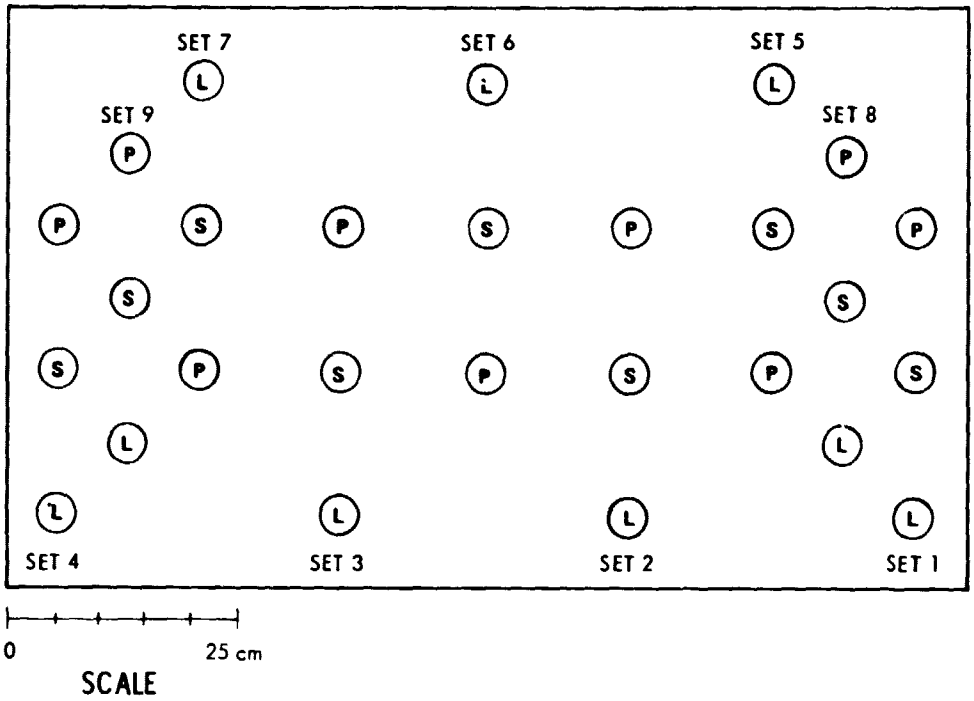

FIGURE A-2. AMTV ARRAY SENSOR LAYOUT

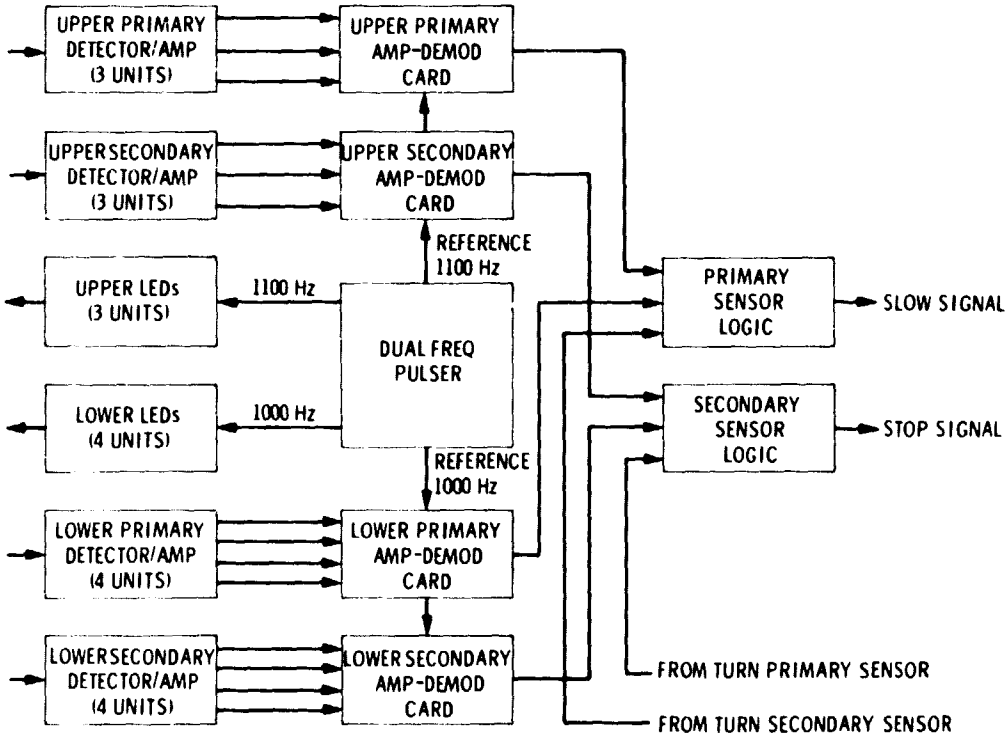

FIGURE A-3. ARRAY SENSOR BLOCK DIAGRAM

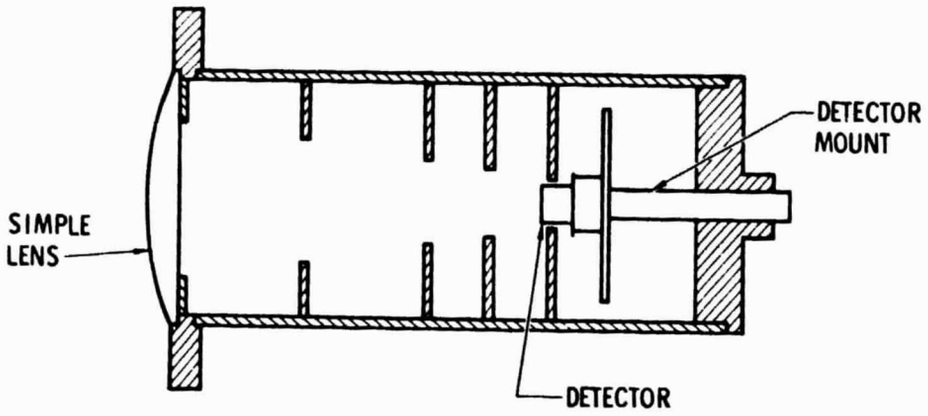

FIGURE A-4. TYPICAL OPTICAL ELEMENT OF ARRAY SENSOR. DETECTOR AND LED ELEMENTS ARE IDENTICAL

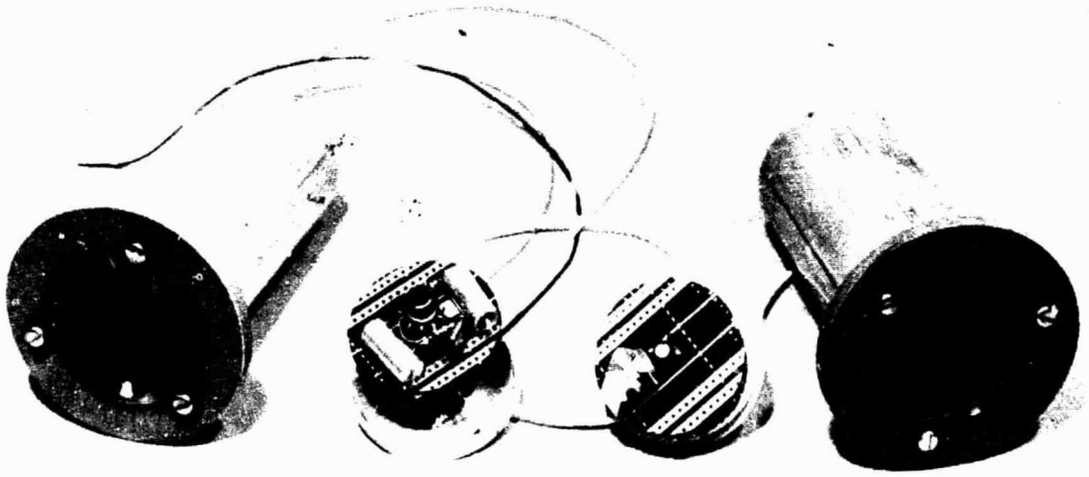

FIGURE A-5. DETECTOR-AMPLIFIER AND LED UNITS

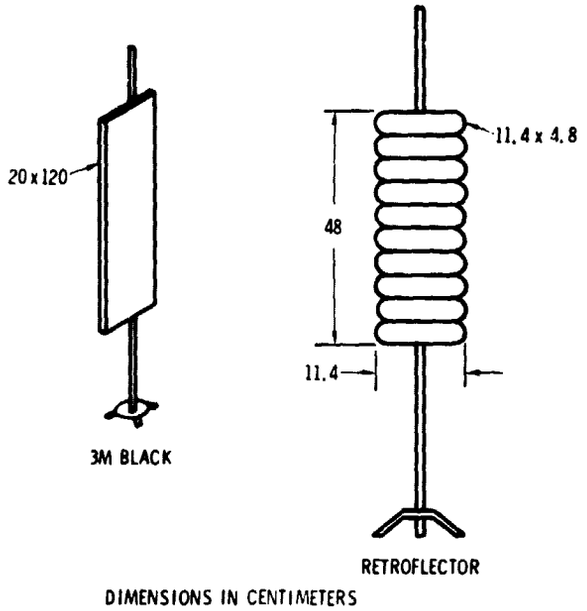

FIGURE A-6. TEST TARGETS

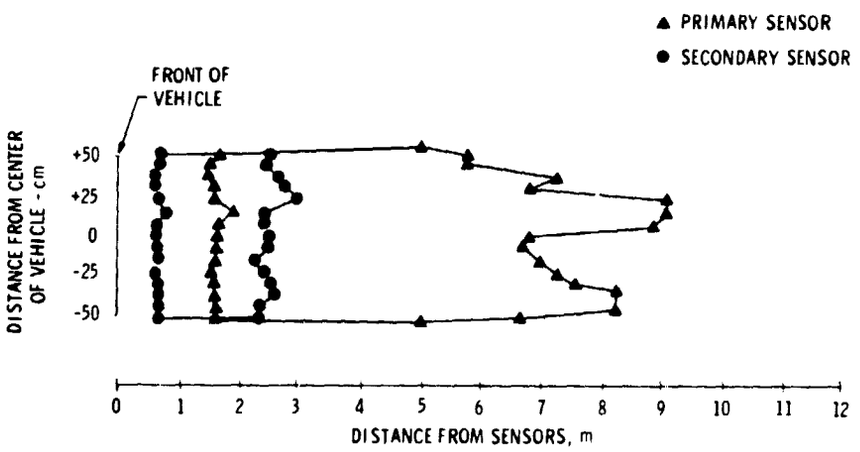

FIGURE A-7. THRESHOLD PATTERN USING BLACK TARGET AND GEOMETRICAL ADJUSTMENT TECHNIQUE

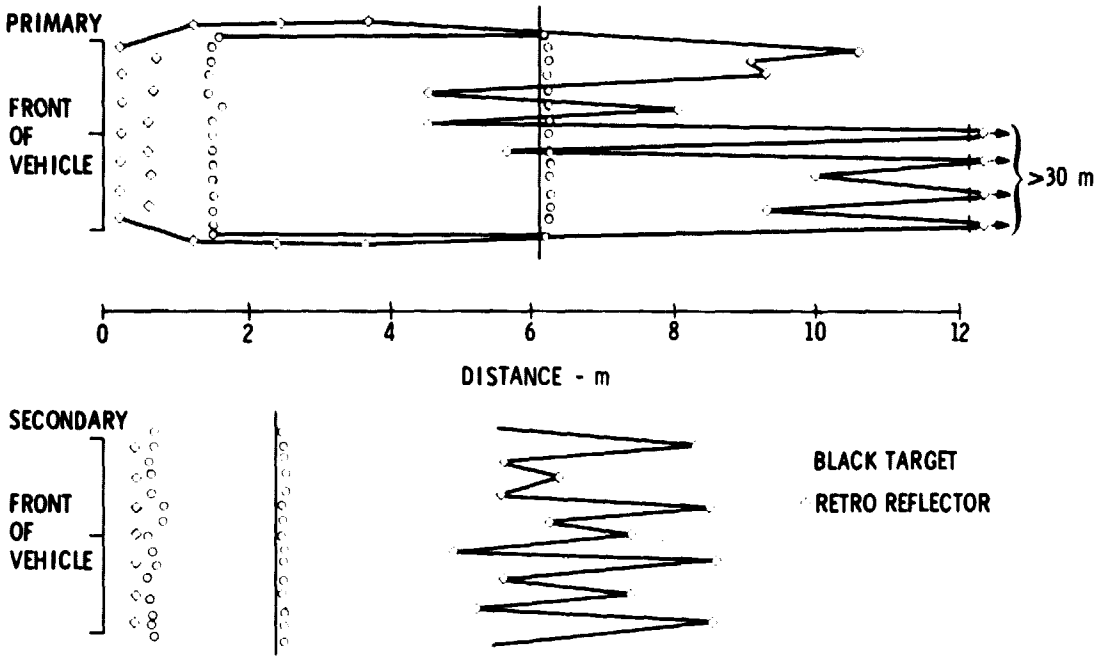

FIGURE A-8. THRESHOLD PATTERN FOR ARRAY SENSOR AFTER ADJUSTMENT FOR UNIFORM THRESHOLD DISTANCE FOR THE BLACK TARGET. BOTH PRIMARY AND SECONDARY SENSOR PATTERNS ARE SHOWN

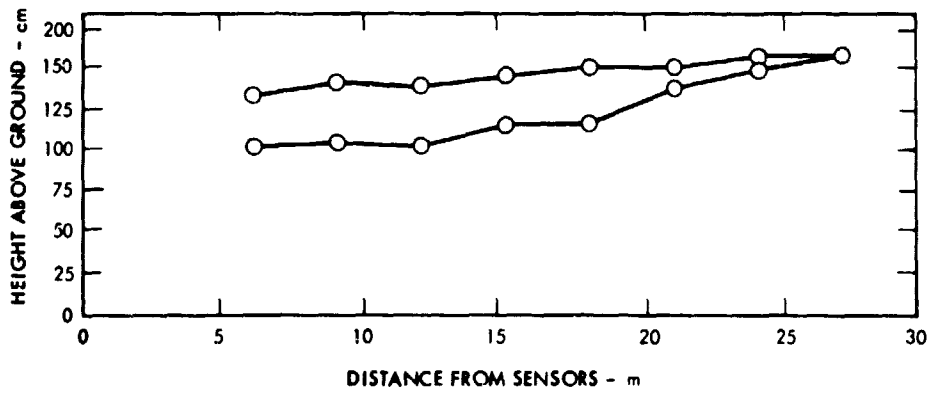

FIGURE A-9. SIDE VIEW OF THRESHOLD PATTERN OF A PRIMARY SENSOR FOR RETROREFLECTOR TARGET (HORIZONTAL POSITION)

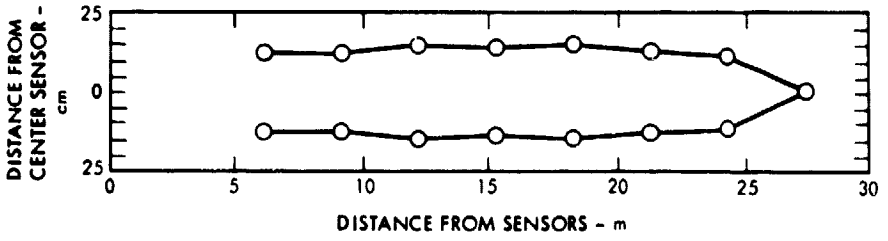

FIGURE A-10. TOP VIEW OF THRESHOLD PATTERN OF A PRIMARY SENSOR FOR THE RETROREFLECTOR (VERTICAL POSITION)

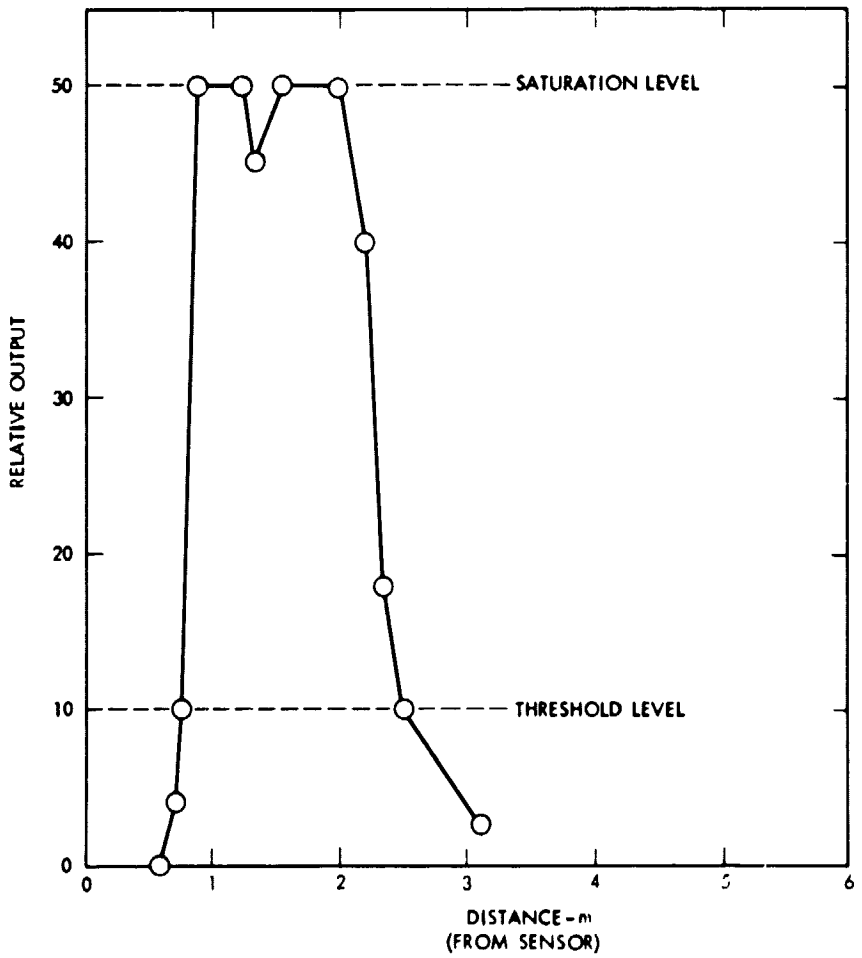

FIGURE A-11. OUTPUT OF THE CENTER SECENDARY SENSOR FOR THE BLACK TARGET

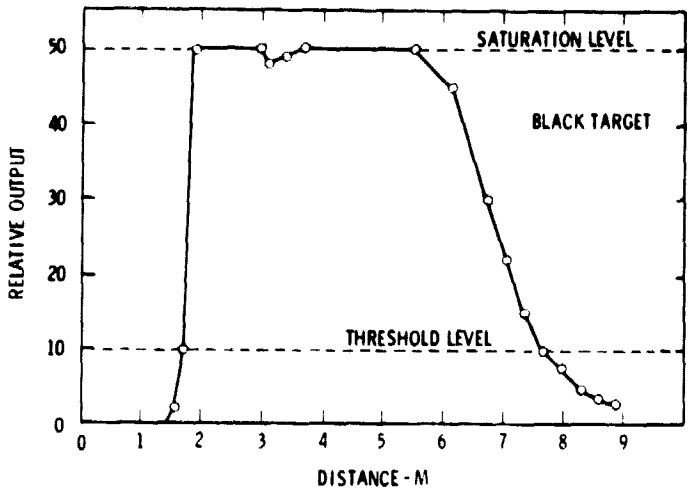

FIGURE A-12. OUTPUT OF THE PRIMARY SENSOR SET VERSUS DISTANCE FOR BLACK TARGET

APPENDIX B

CRUISE-TURN AND U-TURN SENSOR DESIGN

CRUISE TURN SENSOR

Two cruise-turn sensor elements were provided, a right turn set aligned with its axis 8° to the right (Set 8 in Fig. A-1) and a left turn set with its axis 8° to the left (Set 9). Each element is identical to one of the straight-ahead sensor elements. These sensors were activated manually for testing, but ultimately would be enabled by road-fixed signals.

The optical units and the amplifier-demodulator cards of the turn sensors are identical to those in the array sensor and the beam patterns are the same as the array sensor. The LED drive signal is supplied from the 1000 Hz driver in the array sensor (Figure B-1). The turn sensor is activated by applying power to the appropriate LED. The output signal is logically OR'ed in the array sensor logic card.

U-TURN SENSOR

The U-Turn sensor tested was a single fan-beam optical proximity sensor adapted from the first-generation secondary sensor. It has cylindrical lenses that widen its viewing angle. The threshold pattern is shown in Figure B-2. The unit is complete with its own pulser and is also activated by switching on the pulser power to the LED. The connection of the output to the system logic was similar to that of the cruise-turn sensor. The location on the AMTV and the orientation of both the cruise and U-turn sensor are shown in Figure B-3.

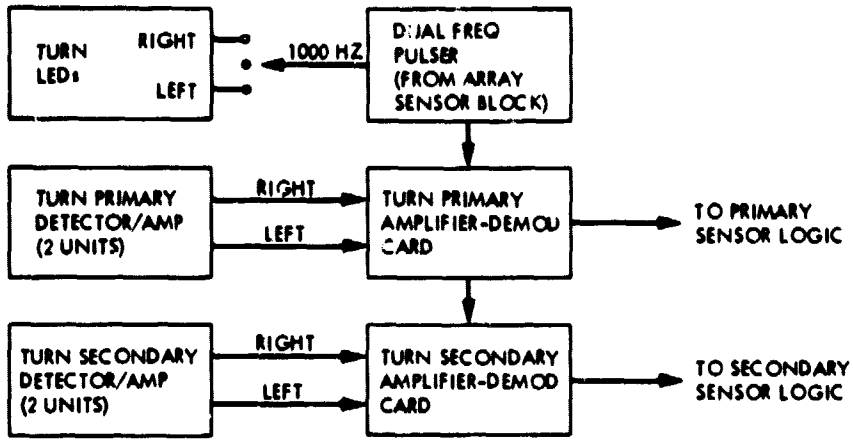

FIGURE B-1. TURN SENSOR

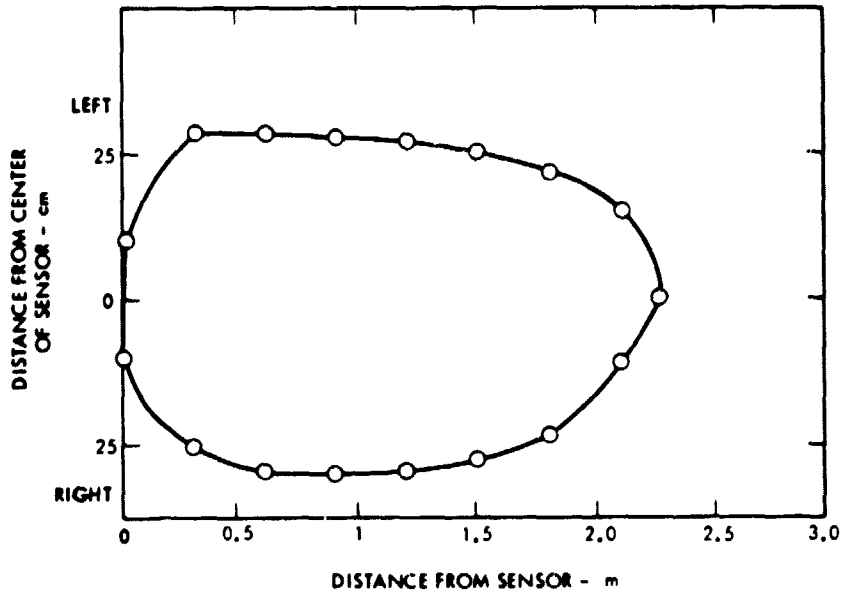

FIGURE B-2. THRESHOLD PATTERN FOR U-TURN SENSOR (SHORT CABLE).
TARGET: 20 cm x 1.22 m, GRAY

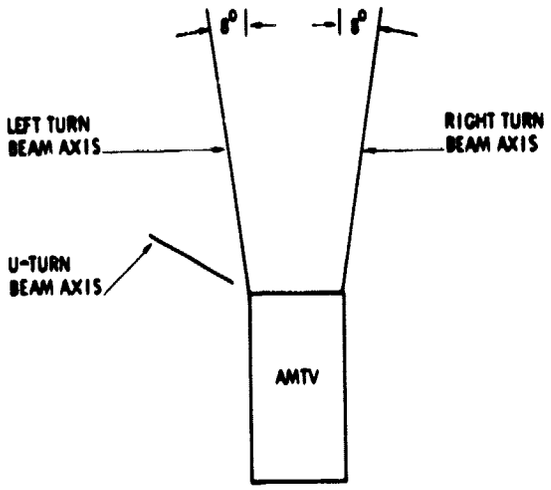

FIGURE B-3. TURN AND U-TURN SENSOR POSITIONS AND VIEWING ANGLES

APPENDIX C

ANALYSIS OF SENSOR SIGNAL POWER AND NOISE

In this section we calculate the signal output of one array sensor element and its noise output for a test case. The results are then compared to the measured signal to noise ratio to determine if the observed performance approximates theoretical expectations. The test case selected is a worst case situation, in which the target is a flat black surface, and the noise is observed for a white diffusely reflecting surface in full sunlight. Curves are also given which indicate light power requirements and signal to noise figures for an optical sensing device.

The geometry used in the calculation is shown in Figure C-1, while Table C-1 defines symbols used below. The radiant energy from the LED illuminates the area A_{st} at the target, where A_{st} is understood to refer to the area of the illuminated spot if the target is oriented normal to the beam ($\theta=0$). Taking into account the geometry, the radiant power collected by the detector is:

$$P_d = \frac{t_i t_f \rho_B P A_d \cos\theta}{\pi d^2} \tag{1}$$

in terms of the total power P in the source beam, provided the field of view of source and detector are identical. The detector output signal is then simply

$$I_{sig} = G R P_d \tag{2}$$

where R is the responsivity of the silicon detector and G is the gain of the electronics to the measurement point.

Similarly, the RMS noise signal current is given by

$$I_n = G \left(2e R P_{sol} \Delta f\right)^{1/2} \tag{3}$$

assuming that the dominant noise is from the solar background P_{sol}. Substituting for the solar background power P_{sol} in (3) we obtain:

$$I_n = G\left(\frac{2e R \phi_{sol} \rho_w t_i t_f \cos\alpha A_d A_{dt} \Delta f}{\pi d^2}\right)^{1/2} \tag{4}$$

Here, I_n is measured at the same point as I_{sig}.

Taking the ratio, to obtain the VSNR ratio at the detector output, and making a minor modification to allow for different source and detector field of view, we obtain:

$$\beta = \frac{I_s}{I_n} = \left(\frac{R\, t_\ell t_f\, A_{dt} A_d}{2\pi e\, \rho_w \phi_{sol}\, \Delta f\, A_{st}^2 \cos\alpha} \right)^{1/2} \frac{\rho_B\, P \cos\theta}{d} \qquad (5)$$

for

$$A_{ST} > A_{DT}$$

and

$$\beta = \left(\frac{R\, t_\ell t_f A_d}{2\pi e\, \rho_w P_{sol}\, \Delta f\, A_{dt}} \right)^{1/2} \frac{\rho_B\, P \cos\theta}{d} \qquad (6)$$

for

$$A_{st} \leq A_{dt}$$

These expressions are quite general and are used to generate theoretical signal to noise curves for proximity sensors, laser scanners and LRF devices in a following paragraph.

Using the numerical values for our AMTV, which are given in Table C-1, and Equation (6) for the signal to noise, one obtains $\beta = 7$.

In order to obtain an experimental value of β for comparison, measurements were made of signal and noise separately. The signal measurements were taken by blocking all the LED's except one and placing the 3-M black target at 5 meters (maximum beam overlap). This measurement was performed inside a building with the lights off. The source power was measured with a commercial radiant power meter.

The noise measurements were taken by positioning a white sheet at a 5 meter distance such that diffuse reflection from the sun would be directed into the detectors. The noise measurement was taken with the sun nearly directly overhead on a clear day. The solar angle of incidence on the white sheet was 45°, and was taken into account.

The measurements yielded $\beta = 5$, in satisfactory agreement with the theoretical calculation. These results confirm that shot noise from background light is dominant, and that the array sensor electronics do not introduce a significant amount of excess noise.

A number of curves are presented in Figures C-2 to C-5 which summarize the theoretical results, and are applicable to any sensor using the

geometry of Figure C-1, which can also include laser scanners or laser range finders. The parameters chosen for each case are as indicated in Table C-2. Source and detector fields of view are assumed to be equal.

In Figure C-2, the power returned to the detector is plotted. Figure C-3 indicates the source power that would be required to achieve a signal-to-noise ratio (VSNR) of 10 at the analog output of the detector. A silicon detector with a responsivity R=0.5 a/w is assumed. The noise source is assumed to be the solar background on a white surface normal to the sun. The solar background is assumed to be restricted to the range from 0.9 μm to 1.1 μm, as it would if it passed through a sharp cut-off filter at 0.9 μm. The 1.1 μm cutoff comes from the silicon detector. The parameters assumed are representative of a proximity sensor.

Figure C-4 shows the power required under similar assumptions for varying signal channel bandwidth. A target distance of 10 m was assumed, and other parameters are appropriate for a scanned laser beam. If detection is to be in real time, spot by spot (no detector integration time between data points), then the bandwidth given is the same as the scanning rate in terms of spot areas examined per second.

Figure C-5 shows the power required from a typical pulsed laser rangefinder source. A detection time constant of 1 ns is assumed, appropriate for obtaining one distance datum from each detected pulse. All other assumptions are as before. Note that peak power from the source is plotted. Average power is lower by the pulse duty factor, typically 10^{-4}.

TABLE C-1. Notation and Values of Parameters Used for Calculation of Signal and Noise Outputs

SYMBOL		QUANTITY	MAGNITUDE	UNIT
A_d	-	Detector collecting lens area	12.5	cm^2
A_{st}	-	Area of source field of view projected on surface normal to axis	201	cm^2
A_{dt}	-	Area of detector field of view (projected)	201	cm^2
d	-	Distance of lens to target	503	cm
e	-	Electronic charge	1.6×10^{-19}	coul
Δf	-	Bandwidth, $1/2\ \pi\ \tau$	1.59 hz	
Φ_{sol}	-	Radiant flux density from the sun between $\lambda = 0.9$ and $1.1\ \mu m$	9.7	mW cm^{-2}
P	-	Total average power from LED source	0.25	mW
P_{sol}	-	Total detected solar power		
P_d	-	Light power collected onto detector		
ρ_B	-	Reflectivity of black target	1×10^{-2}	
ρ_W	-	Reflectivity of white surface	0.9	
R	-	Responsivity of photodiode	0.5	A/W
t_f	-	Transmittance of filter within its pass band	0.8	
t_ℓ	-	Transmittance of lens	0.8	
τ	-	Time constant of detector electronics	0.11	sec
θ	-	Angle of incidence, black target	0	deg
α	-	Solar angle of incidence, white target	45	deg
G	-	Gain of electronics		
I_{sig}	-	Detector signal current		

Table C-2. Parameters Used in Figures C-2 Through C-5

Parameter	Symbol	Fig. C-2	Fig. C-3 Proximity Sensor	Fig. C-4 Laser Scanner	Fig. C-5 Laser Range-finder	Unit
Sensor angle of incidence	θ	0	0	0	0	
Solar angle of incidence	α	0	0	0	0	
Lens transmittance	t_ℓ	1	1	1	1	
Filter transmittance	t_f	1	1	1	1	
Target reflectivity	ρ_B	.01	.01	.01	.01	
Detection time constant	τ	-	0.1	Variable	10^{-9}	sec
Background reflectivity	ρ_w	1	1	1	1	
Solar irradiance	$\dot{\psi}_{sol}$	9.7	9.7	9.7	9.7	mw/cm^2
S/N	β	-	10	10	10	

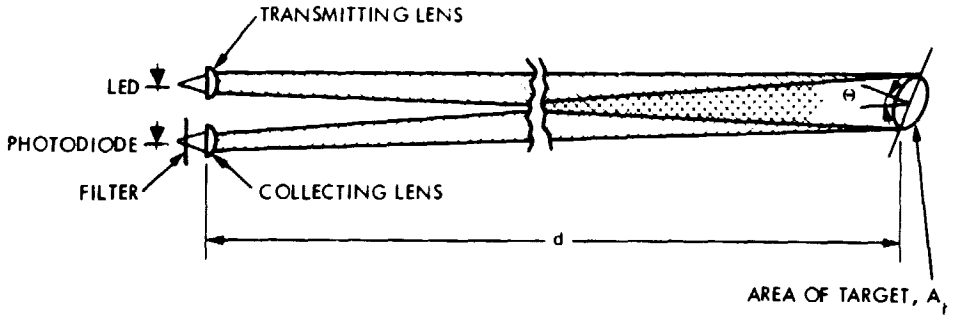

FIGURE C-1. GEOMETRY OF OPTICAL SENSING SYSTEM

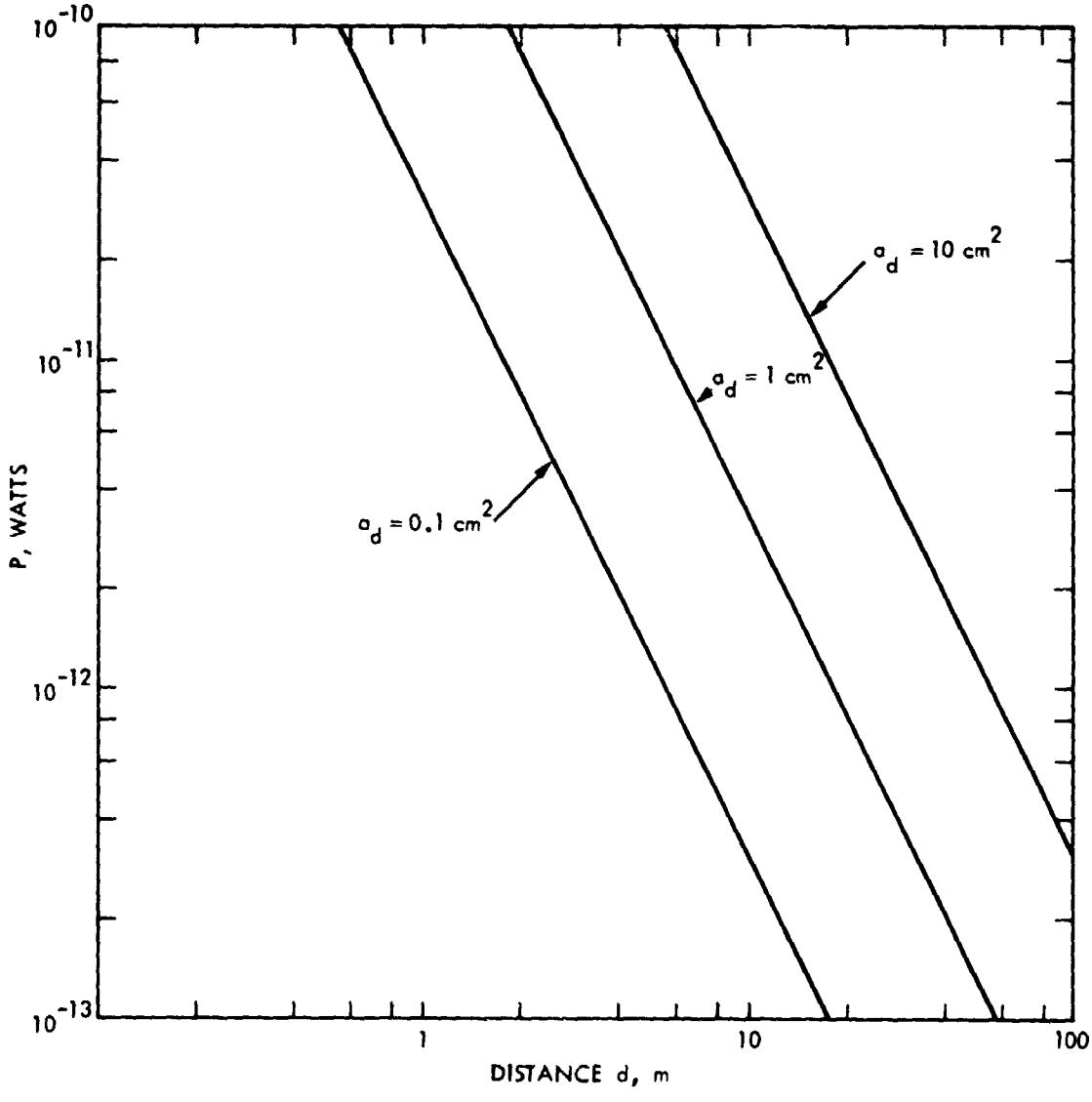

FIGURE C-2. DETECTED SIGNAL POWER VERSUS DISTANCE AND COLLECTING LENS AREA, FOR 1 mW ILLUMINATION

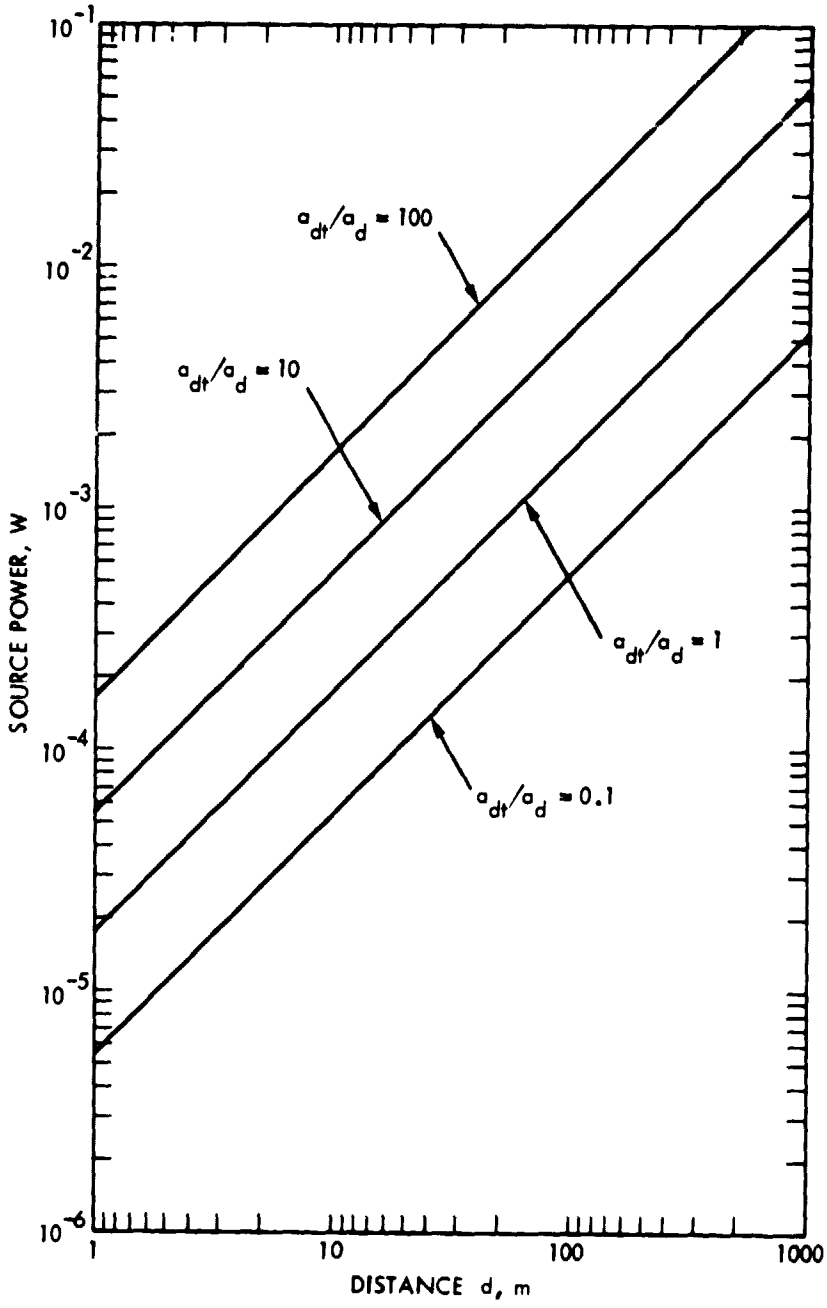

FIGURE C-3. SOURCE POWER REQUIRED FOR A VSNR OF 10 AS A FUNCTION OF DISTANCE; COLLECTING LENS AREA AND FIELD OF VIEW PARAMETERS. DETECTION TIME CONSTANT = 0.1 sec

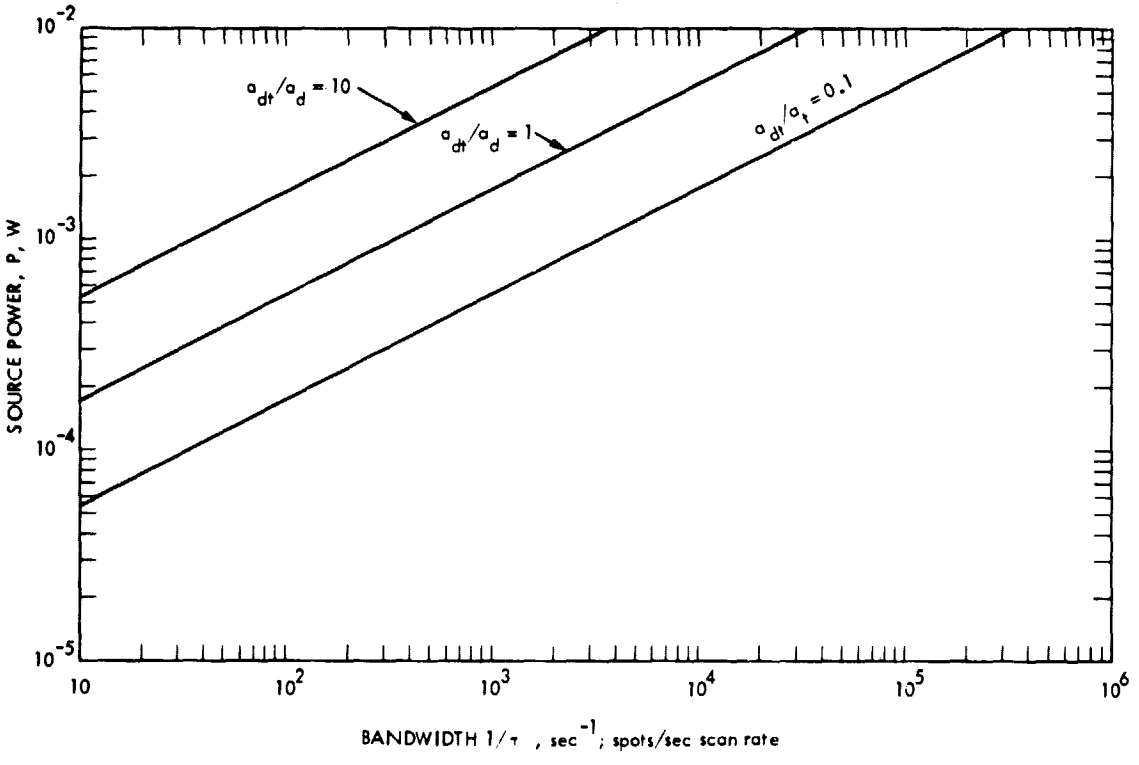

FIGURE C-4. SOURCE POWER REQUIRED AS A FUNCTION OF BANDWIDTH, OR SPOTS SCANNED PER SECOND, FOR A LASER SCANNER

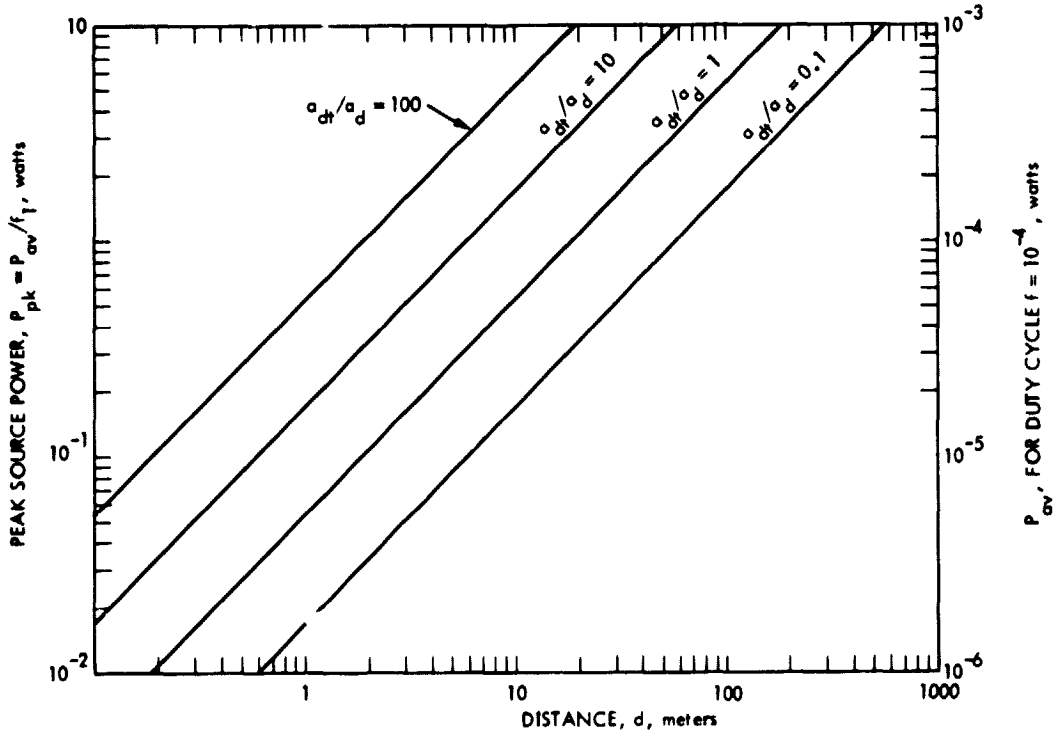

FIGURE C-5. PEAK SOURCE POWER REQUIRED AS A FUNCTION OF DISTANCE, WITH COLLECTOR AREA AND FIELD OF VIEW AS PARAMETERS. DETECTION TIME CONSTANT IS ASSUMED TO BE 1 ns, TYPICAL OF A PULSED LASER RANGE FINDER

APPENDIX D

ULTRASONIC SENSOR DESIGN AND FUNCTIONAL CHARACTERISTICS

For the purpose of evaluating ultrasonic sensing a Polaroid Pronto Sonar Land Camera was purchased. The sonic ranging elements were removed and interfaced with conventional digital electronics to display range in meters or feet. The electronic interface is described and the observed ranging characteristics of the ultrasonic transducer are presented.

CIRCUIT DESCRIPTION

The pronto camera Sonar Module Board provides randing information from two output lines, one of which goes low when the ranging pulse is sent and the other goes low when the reflected sound pulse is received. A system block diagram of the interface we designed to test the sensor is shown in Figure D-1. A low frequency square-wave oscillator periodically powers the Sonar Module Board (SMB). The oscillator is built from CMOS Schmitt trigger which allows the SMB to power up once every 0.1 second to once every 5 seconds. There is some internal resetting before an ultrasonic pulse is sent from the transducer. In about 5 msec after the SMB is powered, the transmit pin on the SMB goes low, coinciding with the ultrasonic pulse being sent. The receive pin remains high until the return is detected. Because noise from the transducer driver can be seen on the transmit, receive, and power lines, negative edge detection was used in the wave form shaping block in order to obtain cleaner waveforms. These signals are combined to yield a single level signal which remains high for the out and back travel time of the sound wave. The level signal is then used in the counter control logic to gate pulses from an oscillator into counters for display. Note that there is no need for latching as ranging information is acquired in a maximum of 50 msec. This is the default value of the sensor when it is pointed to the sky (about 9 meters).

The electronics described above have been placed in an aluminum box 7.6 x 10.2 x 12.7 cm. The displays are TTL type counters and 7 segment decoders/drivers and because of this, consume a large amount of power. Thus the power source is external and can be any type 10-30 volt capable of sourcing 500 ma (e.g., Eveready No. 732, 12 VDC lantern battery.)

TESTED CHARACTERISTICS

Test Description

The sensor was placed on a rotatable bench and aimed at a stationary target in order to plot the threshold, the boundary between sensing the target and not sensing it. The target was then placed at different distances and the process of sweeping repeated. Two different targets were used. One was the 20 cm wide wooden target used for testing the existing IR sensors on the JPL AMTV. The second target was a 1.3 cm diameter standing rod. These tests were performed indoors in a benign environment and outdoors in a 0-16 kph, slightly gusty wind. Testing was also done to observe the

effects of reflections from road surfaces. This was done by placing the sonar box parallel to the road surface and rotating the box down until the sonar sensed the road.

Test Results and Observations

The sensitive area for an 20-cm black target and a 1.3-cm standing rod is shown in Figures D-2 and D-3. The solid line represents 100% detection and the dotted line represents about 10% detection. The slight wind that was present when the outdoors data was taken did not appear to present much of a problem. The response to a road surface was quite remarkable. When the transducer emits parallel to the ground, the sonar box can be placed on the ground and still does not sense it. Figure D-4 shows a graph which plots height above the ground vs the angle at which the sensor must be pointed to sense the ground. Results are shown for different road surfaces. No comprehensive test was performed to analyze the sensitivity of the sensor to ambient noises in order to determine what kind of misranging the sonar might do. However, no indication was seen that the sensor would malfunction in a typical automotive environment Dense rainfall did not affect the operation of the device.

The sonar emits a 1 msec pulse of 50, 53, 57, and 60 kHz ultrasonic acoustic energy. These frequencies are inaudible, but the 1 msec pulse envelop contains frequency components which can be heard and thus each ranging sample can be heard as a weak click. Also, when the sonar is operating at a high sample rate in an enclosed room, a certain amount of pressure can be felt on the ear.

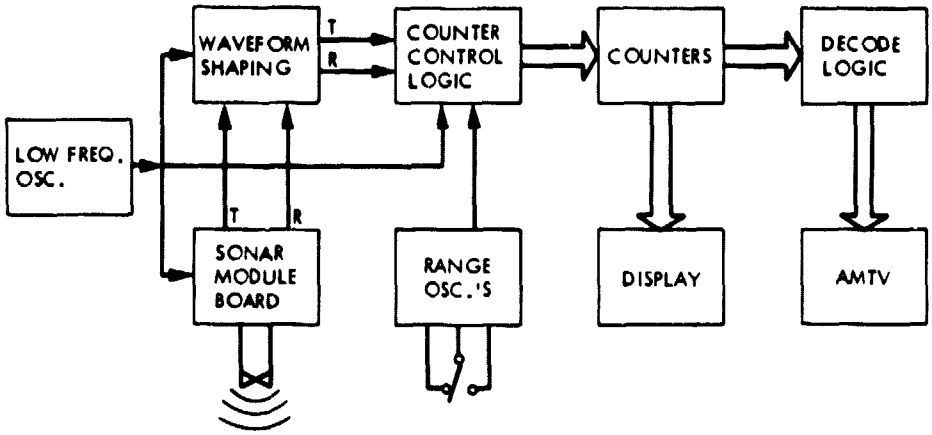

FIGURE D-1. PRONTO SMG AND INTERFACE BLOCK DIAGRAM

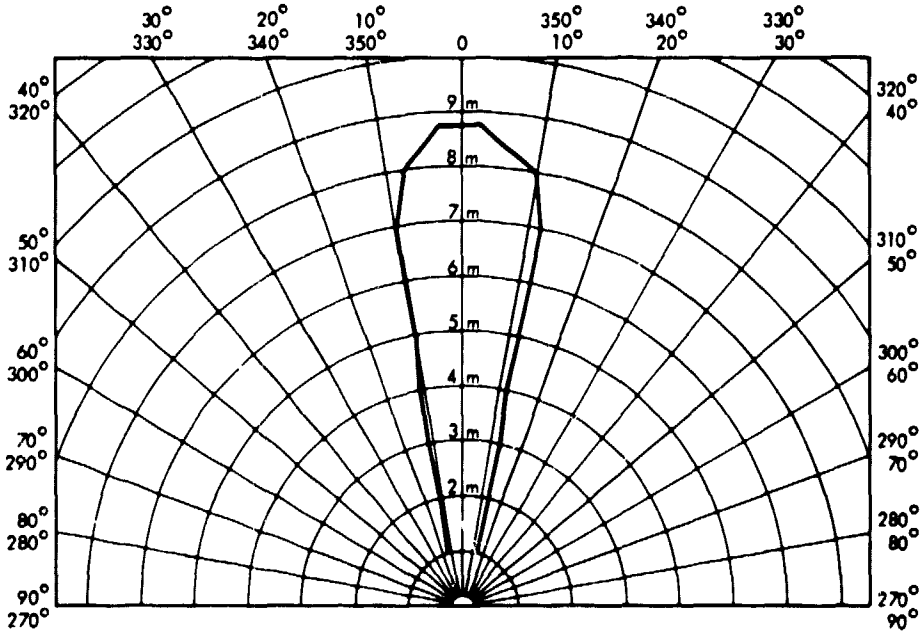

FIGURE D-2. DETECTION THRESHOLD PATTERNS FOR ULTRASONIC SENSOR USING 20-cm WIDE WOOD TARGET

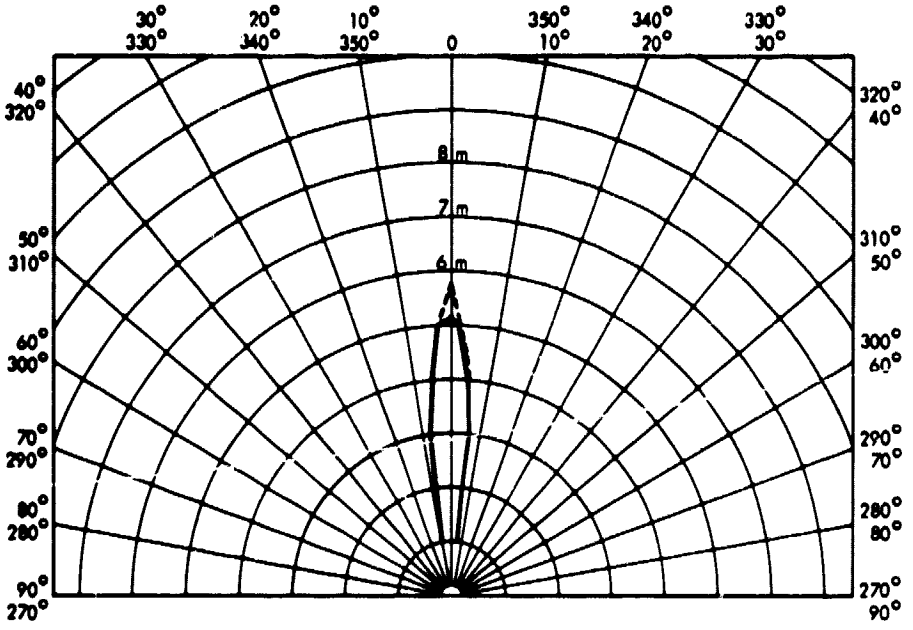

FIGURE D-3. DETECTION THRESHOLD PROFILE FOR ULTRASONIC SENSOR USING 1.3-cm DIAMETER STEEL ROD TARGET

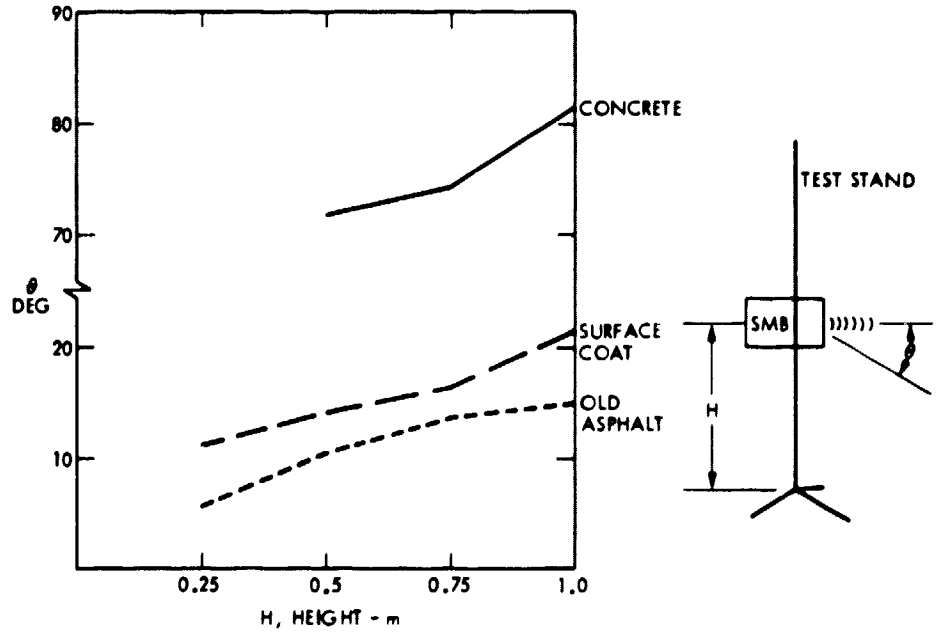

FIGURE D-4. GRAPH SHOWING THE ANGLE MEASURED FROM HORIZONTAL AT WHICH THE SENSOR FIRST DETECTS A PAVED SURFACE

REFERENCES

1-1. Johnston, Alan R., Peng Ted, K.C., Vivian, Howard C., and Wang, Peter K. "AMTV Technology and Safety Study," UMTA-CA-06-0088-78-1, Feb. 1978.

1-2. Herridge, J.T., Design of Pedestrian Protection in the JPL Automated Mixed Traffic Vehicle, Battelle Columbus Laboratories, Sept. 14, 1979.

2-1. Meisenholder, G.W., and Johnston, A.R., "Control Techniques for an Automated Mixed Traffic Vehicle," Proceedings, Joint Automatic Control Conference, p. 421, San Francisco, June 1977.

2-2. Meisenholder, G.W., and Johnston, A.R., :Automated Mixed Traffic Vehicle Status." Proceedings, Automated Guideway Transit Conference, UMTA, Cambridge, Mass, Feb. 1978.

4-1. Tippins, H.H., and Johnston, A.R., Application of Multiple Detector Arrays to Optical Proximity Sensors, JPL Internal Report 760-128, Aug. 1975.

4-2. Nilsson, N.J., "A Mobile Automation: An Application of Artifical Intelligence Techniques," Proceedings of the First International Conference on Artificial Intelligence, pp. 509-520, ACM, May 1969.

4-3. Agin, G.J. and Binford, T.O., "Computer Description of Curved Objects," Proceedings of the Third International Joint Conference on Artificial Intelligence, Stanford University, Stanford, Ca., 20-23 August, 1973.

4-4. Yatabe, T., Hirose, T., Tsugawa, S. and Matsumoto, S. "Driving Control Method for Automated Vehicle with Artificial Eye," Annual Conference Proceedings, Industrial Applications of Microprocessors, IECI 78: Philadelphia PA Mar. 20-22, 1978, pp. 29-35.

4-5. Yakimovsky, Y. and Cunningham, R., "A System for Extracting Three-dimensional Measurements from a Stereo Pair of TV Cameras" Computer Graphics and Image Processing, 7, 195 (1978).

4-6. Kuriger, William L, "A Proposed Obstacle Sensor for a Mars Rover" J. Spacecraft & Rockets 8 1043 (1971).

4-7. Lewis, R.A., and Johnston, A.R., "A Scanning Laser Rangefinder for a Robotic Vehicle", Proceedings International Joint Conference on Artificial Intelligence, Cambridge, Mass., August 1977; JPL TM 33-809.

4-8. Mamon, G., Youmans, D.G., Sztankay, Z.G., and Morgan, C.E. "Pulsed GaAs Laser Terrain Profiler" Appl. Optics. 17, 868 (1978).

4-9. Macovski, Albert, "Ultrasonic Imaging Using Arrays" Proc IEEE 67, 484 (1979).

4-10. Wood, L.E., Chandler, R.A., and Warner, B.D., "Analysis of Problems in the Application of Radar Sensors to Automobile Collision Prevention," NHTSA/DOT-HS-314-3-601 Dec. 1973.

5-1. Herridge, J.T., and Pritz, H.B., "A Study of the Dynamics of Pedestrians and Generally Unsupported Traffic System Occupants in Selected Accident Modes", Proceedings of 17th Conference of the American Association for Automotive Medicine, Oklahoma City, Oklahoma, November 14-17, 1973.

5-2. Pritz, H.B., Hassler, C.R., Herridge, J.T., Weis, E.B. Jr., "Experimental Study of Injury Minimization Through Vehicle Design", 19th Stapp Car Crash Conference, San Diego, California, 1975.

5-3. Pritz, H.B., Hassler, C.R., and Weis, E.B., "Pedestrian Impact: Baseline and Preliminary Concepts Evaluation", Final Technical Report of Contract DOT-HS-00961, Report No. DOT-HS-803 817, May 1978.

5-4. Pritz, H.B., "Vehicle Design for Pedestrian Protection", The Seventh International Technical Conference on Experimental Safety Vehicles, Paris, June 5-8, 1979.

5-5. Trosien, K.R., and Patrick, L.M., Wayne State University, "Windshield Injury Potential as a Function of Windshield Installation Method", SAE Paper No. 700430, 1970 International Automobile Safety Conference Compendium, Detroit, Michigan, May 13-15, 1970.

5-6. Lucchini, E., and Weissner, R., Volkswagenwerk AG, "Results From Experimental Simulations of Car-to-Pedestrian Collisions With VW-Production Cars", The Seventh International Technical Conference on Experimental Safety Vehicles, Paris, June 5-8, 1979.